Supplementary Information (SI) for Inorganic Chemistry Frontiers.
This journal is © the Partner Organisations 2026

Supporting Information

1D Anionic Dysprosium(III) Coordination Polymers with Photoactive Protonated 4-Styrylpyridinium Counter-Ions: Photoinduced Modulation of Magnetic Behavior *via* Synergistic Dual Photoresponses

Shi-Kun Yan,[†a] Yu-Hang Wang,[†a] Yan-Rui Zhao,[a] Jin Zhang,[a] Qi-Yue Xin,[a] Ya-Hui Wang,[a] Guang-Zhi Zhou,[a] Ai-Huan Sun,*[b] Ji-Xiang Hu,*[a, c] Guo-Ming Wang*[a]

[a]*Department College of Chemistry and Chemical Engineering, Qingdao University, Shandong, 266071, China*

[b]*Department College of Chemistry and Chemical Engineering, Taishan University, Taian, 271000, China*

[c]*State Key Laboratory of Fine Chemicals, Dalian University of Technology, Dalian 116024, China*

Contents

Table S5. Continuous Shape Measure (CShM) analyses of geometries for **1-Dy** and by SHAPE 2.0 Software.

Table S6. Continuous Shape Measure (CShM) analyses of geometries for **2-Dy** and by SHAPE 2.0 Software.

Table S7. Continuous Shape Measure (CShM) analyses of geometries for **3-Dy** and by SHAPE 2.0 Software.

Table S8. Details of Hydrogen Bond Interactions in **1-Dy** at 150 K.

Table S9. Details of Hydrogen Bond Interactions in **2-Dy** at 150 K.

Table S10. Details of Hydrogen Bond Interactions in **3-Dy** at 150 K.

Table S11 The Cole-Cole fitting parameters of **3*-Dy** from 7.6 K to 9.1 K based on the generalized Debye law.

Measurements:

Elemental analyses (for C, H, and N) were performed on a Perkin-Elmer 240C analyzer (Perkin-Elmer, USA). The thermogravimetric (TG) analyses were performed under a N_2 atmosphere on a Rigaku standard TG-DTA (differential thermal analysis) analyzer. IR curves for all compounds were measured on a FT-IR spectrometer (MAGNA-560 (Nicolet)) at room temperature with KBr pellets. The time-dependent luminescence spectra were performed on a Hitachi F-4700 Fluorescence spectrometer. The UV-Vis spectrometer was recorded on a Puxi Tu-1901 spectrophotometer using $BaSO_4$ as a reference. The room temperature EPR spectroscopy was recorded on a CIQTEK EPR200-Plus with continues-wave X band frequency. ^{1}H NMR spectra were recorded on a JNM-ECZ600R/S1 400 MHz spectrometer in DMSO-d_6 at room temperature. The magnetic susceptibility measurements of the samples were recorded on a Quantum Design MPMS magnetometer. All data were corrected for diamagnetic contributions from the eicosane and core diamagnetism estimated using Pascal's constants. Powder X-ray diffraction (PXRD) spectra were performed through Rigaku standard MiniFlex600 and HyPix diffractometers. Simulation of the PXRD curve was carried out by the single-crystal data and diffraction-crystal module of the Mercury (Hg) program. A high-power UVLED spot lamp source (HEIGHT-LED, HTLD-4II) (365 nm) were equipped to prepare the photo-responsive experiments.

Experimental

Synthesis of Me-4-arylethene

In a 100-mL flask, triethyl phosphite (15 mmol) and 4-methylbenzyl chloride (15 mmol) were combined and stirred under reflux for 4 hours. After cooling the reaction mixture to room temperature without isolating the intermediate 4-methylbenzyl triethyl phosphite, pyridine-4-carbaldehyde (12 mmol) and tetrahydrofuran (THF, 20 mL) were added sequentially. Sodium hydride (NaH, 45 mmol) was then introduced gradually under ice-water cooling. The resulting mixture was heated under reflux for 1 hour. Upon completion, the reaction was cooled to room temperature and poured into a beaker containing 100 mL of ice-water under vigorous stirring. Solid precipitates formed immediately, which were collected by filtration and subsequently recrystallized from anhydrous ethanol. White solid. 58% yield. ^{1}H NMR (400 MHz, DMSO-d_6) δ 8.53 (d, 2H), 7.56-7.49 (m, 4H), 7.23-7.11 (m, 4H), 2.32 (s, 3H).

Synthesis of H-4-arylethene

In a 100 mL flask, triethyl phosphite (15 mmol) and benzyl chloride (15 mmol) were mixed and stirred under reflux for 4 hours. After cooling the reaction mixture to room temperature without isolating the intermediate benzyl triethyl phosphite, pyridine-4-carbaldehyde (12 mmol) and tetrahydrofuran (THF, 20 mL) were added successively. Sodium hydride (NaH, 45 mmol) was then added slowly under ice-water cooling. The resulting mixture was heated under reflux for 1 hour. After completion, the reaction was cooled to room temperature and poured into a beaker containing 100 mL of ice-water under vigorous stirring. Solid precipitates formed immediately, which were collected by filtration and recrystallized from anhydrous ethanol. White solid. 66% yield. ^{1}H NMR (400 MHz, DMSO-d_6) δ 8.54 (t, 2H), 7.67 (t, 2H), 7.57 (t, 3H), 7.42 (t, 2H), 7.34 (t, 1H), 7.27 (d, 2H).

Synthesis of Cl-4-arylethene

In a 100 mL flask, triethyl phosphite (15 mmol) and 4-chlorobenzyl chloride (15 mmol) were mixed and stirred under reflux for 4 hours. After cooling the reaction mixture to room temperature without isolating the intermediate 4-chlorobenzyl triethyl phosphite, pyridine-4-carbaldehyde (12 mmol) and tetrahydrofuran (THF, 20 mL) were added successively. Sodium hydride (NaH, 45 mmol) was then added slowly under ice-water cooling. The resulting mixture was heated under reflux for 1 hour. Upon completion, the reaction was cooled to room temperature and poured into a beaker containing 100 mL of ice-water under vigorous stirring. A solid precipitated immediately, which was collected by filtration and recrystallized from anhydrous ethanol. White solid. 45% yield. ^{1}H NMR (400 MHz, DMSO-d_6) 7.56-7.53 (m, 4H), 7.48-7.43 (m, 2H), 7.35 (d, 2H), 7.17 (t, 1H).

(H-4-Me-4spy)[Dy(H$_2$-HEDP)$_2$] (1-Dy)

(H-4-Me-4spy)[Dy(H$_2$-HEDP)$_2$] (**1-Dy**): Dy_2O_3 (0.0423 g, 0.112 mmol), Me-4-spy (0.0285 g, 0.146 mmol), HEDP (0.0981 g, 0.438 mmol) were dissolved in the mixed solvents of CH_3OH/H_2O (2 mL / 2 mL). The mixture was placed in a 20 mL Teflon-lined glass vial, and heated at 90 °C for 4 days. The Crystals were obtained after slowly cooling the mixture for 24 h at room temperature. Yield: ca. 25% based on Dy_2O_3. Elemental analysis for **1-Dy** (%): calcd for $C_{18}H_{24}NO_{14}P_4Dy$ (764.76): C, 28.24; H,

3.14; N, 1.83. Found: C, 28.22; H, 3.17; N, 1.82. IR of **1-Dy** (KBr pellets, cm^{-1}): 1639(s), 1507(s), 1449(w), 1147(s), 1054(w), 978(s), 903(m), 814(s), 755(s), 721(m), 690(w), 640(s), 534(m), 448(m). **1*-Dy** was obtained by Xe-lamp irradiation of compound **1-Dy** at room temperature for 60 min. For complex **1*-Dy** (%): calcd for $C_{18}H_{24}NO_{14}P_4Dy$ (764.76): C, 28.24; H, 3.14; N, 1.83. Found: C, 28.25; H, 3.13; N, 1.84. IR of **1*-Dy** (KBr pellets, cm^{-1}): 1621(w), 1508(s), 1445(w), 1147(s), 1055(w), 918(m), 646(s), 538(m), 448(m).

(H-4-spy)[Dy(H_2-HEDP)$_2$] (2-Dy)

(H-4-spy)[Dy(H_2-HEDP)$_2$] (**2-Dy**): Dy_2O_3 (0.0423 g, 0.112 mmol), 4-spy (0.0265 g, 0.146 mmol), HEDP (0.0981 g, 0.438 mmol) were dissolved in the mixed solvents of CH_3OH/H_2O (2 mL / 2 mL). The mixture was placed in a 20 mL Teflon-lined glass vial, and heated at 90 °C for 4 days. The Crystals were obtained after slowly cooling the mixture for 24 h at room temperature. Yield: ca. 37% based on Dy_2O_3. Elemental analysis for **2-Dy** (%): calcd for $C_{17}H_{24}NO_{14}P_4Dy$ (752.75): C, 27.10; H, 3.19; N, 1.86. Found: C, 27.13; H, 3.21; N, 1.83. IR of **2-Dy** (KBr pellets, cm^{-1}): 1639(s), 1507(s), 1449(w), 1147(s), 1054(w), 978(s), 903(m), 814(s), 755(s), 721(m), 690(w), 640(s), 534(m). **2*-Dy** was obtained by Xe-lamp irradiation of compound **2-Dy** at room temperature for 60 min. For complex **2*-Dy** (%): calcd for $C_{17}H_{24}NO_{14}P_4Dy$ (752.75): C, 27.10; H, 3.19; N, 1.86. Found: C, 27.11; H, 3.19; N, 1.84. IR of **2*-Dy** (KBr pellets, cm^{-1}): 1639(s), 1507(s), 1449(w), 1144(w), 1054(w), 903(m), 814(s), 732(m), 702(s), 640(s), 534(m).

(H-4-Cl-4spy)[Dy(H_2-HEDP)$_2$] (3-Dy)

(H-4-Cl-4spy)[Dy(H_2-HEDP)$_2$] (**3-Dy**): Dy_2O_3 (0.0423 g, 0.112 mmol), Cl-4-spy (0.0316 g, 0.146 mmol), HEDP (0.0981 g, 0.438 mmol) were dissolved in the mixed solvents of CH_3OH/H_2O (2 mL / 2 mL). The mixture was placed in a 20 mL Teflon-lined glass vial, and heated at 90 °C for 4 days. The Crystals were obtained after slowly cooling the mixture for 24 h at room temperature. Yield: ca. 52% based on Dy_2O_3. Elemental analysis for **3-Dy** (%): calcd for $C_{17}H_{24}NO_{14}P_4DyCl$ (788.20): C, 25.88; H, 3.04; N, 1.77. Found: C, 25.84; H, 3.08; N, 1.74. IR of **3-Dy** (KBr pellets, cm^{-1}):

1623(s), 1507(s), 1444(w), 1146(w), 1060(w), 978(s), 911(m), 830(s), 644(m), 549(m). **3*-Dy** was obtained by Xe-lamp irradiation of compound **3-Dy** at room temperature for 60 min. For complex **3*-Dy** (%): calcd for $C_{17}H_{24}NO_{14}P_4DyCl$ (788.20): C, 25.88; H, 3.04; N, 1.77. Found: C, 25.83; H, 3.04; N, 1.77. IR of **3*-Dy** (KBr pellets, cm^{-1}): 1635(s), 1494(w), 1150(w), 1054(w), 906(m), 810(s), 765(s), 691(m), 647(s), 593(s), 530(m), 454(m).

(H-4-Me-4spy)[Y(H$_2$-HEDP)$_2$] (1-Y)

(H-4-Me-4spy)[Y(H_2-HEDP)$_2$] **(1-Y).** The synthesis of compound **1-Y** was used by the same method as compound **1-Dy** but using Y_2O_3 (0.045 g, 0.10 mmol). Yield: ca. 35% based on Y_2O_3. Elemental analysis for **1-Y** (%): calcd for $C_{18}H_{24}NO_{14}P_4Y$ (691.17): C, 31.25; H, 3.47; N, 2.02. Found: C, 31.20; H, 3.50; N, 2.01. IR (KBr pellets, cm^{-1}): 1628(s), 1592(s), 1508(s), 1236(w), 1150(w), 1054(w), 978(s), 918(m), 833(m), 645(m), 532(w), 486(w), 406(s). **1*-Y** was obtained by Xe-lamp irradiation of compound **1-Y** at room temperature for 60 min. For complex **1*-Y** (%): calcd for $C_{18}H_{24}NO_{14}P_4Y$ (691.17): C, 31.25; H, 3.47; N, 2.02. Found: C, 31.20; H, 3.50; N, 2.01. IR (KBr pellets, cm-1): 1628(s), 1150(w), 1042(w), 987(s), 938(m), 828(m), 675(m), 549(w), 466(w).

(H-4-spy)[Y(H$_2$-HEDP)$_2$] (2-Y)

(H-4-spy)[Y(H_2-HEDP)$_2$] **(2-Y).** The synthesis of compound **2-Y** was used by the same method as compound **1-Dy** but using Y_2O_3 (0.045 g, 0.10 mmol). Yield: ca. 41% based on Y_2O_3. Elemental analysis for **2-Y** (%): calcd for $C_{17}H_{24}NO_{14}P_4Y$ (679.14): C, 30.04; H, 3.53; N, 2.06. Found: C, 30.03; H, 3.52; N, 2.07. IR (KBr pellets, cm-1): 1620(s), 1505(s), 1449(s), 1148(m), 1066(w), 972(m), 917(m), 814(s), 757(s), 644(s), 524(w), 483(s), 443(w). **2*-Y** was obtained by Xe-lamp irradiation of compound **2-Y** at room temperature for 60 min. For complex **2*-Y** (%): calcd for $C_{17}H_{24}NO_{14}P_4Y$ (679.14): C, 30.04; H, 3.53; N, 2.06. Found: C, 30.05; H, 3.52; N, 2.05. IR (KBr pellets, cm-1): 1617(s), 1505(s), 1449(s), 1148(m), 1066(w), 917(m), 814(s), 757(m), 644(s), 524(w), 483(s), 447(w).

(H-4-Cl-4spy)[Y(H_2-HEDP)$_2$] (3-Y)

(H-4-Cl-4spy)[Y(H_2-HEDP)$_2$] **(3-Y).** The synthesis of compound **3-Y** was used by the same method as compound **1-Dy** but using Y_2O_3 (0.045 g, 0.10 mmol). Yield: ca. 48% based on Y_2O_3. Elemental analysis for **3-Y** (%): calcd for $C_{17}H_{24}NO_{14}P_4YCl$ (715.62): C, 28.51; H, 3.35; N, 1.96. Found: C, 28.54; H, 3.37; N, 1.98. IR (KBr pellets, cm^{-1}): 1634(s), 1502(m), 1149(s), 1060(w), 982(m), 910(s), 810(s), 766(s), 733(s), 690(s), 643(s), 592(s), 540(w), 433(w). **3*-Y** was obtained by Xe-lamp irradiation of compound **3-Y** at room temperature for 60 min. For complex **3*-Y** (%): calcd for $C_{17}H_{24}NO_{14}P_4YCl$ (715.62): C, 28.51; H, 3.35; N, 1.96. Found: C, 28.54; H, 3.37; N, 1.98. IR (KBr pellets, cm^{-1}): 1634(s), 1502(m), 1149(m), 1044(w), 987(s), 934(s), 824(s), 666(m), 531(m), 432(w).

(H-4-Me-4spy)[Gd(H_2-HEDP)$_2$] (1-Gd)

(H-4-Me-4spy)[Gd(H_2-HEDP)$_2$] **(1-Gd).** The synthesis of compound **1- Gd** was used by the same method as compound **1-Dy** but using Gd_2O_3 (0.045 g, 0.10 mmol). Yield: ca. 35% based on Gd_2O_3. Elemental analysis for **1-Gd** (%): calcd for $C_{18}H_{24}NO_{14}P_4Gd$ (759.51): C, 28.44; H, 3.16; N, 1.84. Found: C, 28.42; H, 3.17; N, 1.82. IR (KBr pellets, cm^{-1}): 1627(m), 1508(s), 1448(s), 1150(w), 1054(w), 978(s), 918(m), 833(m), 645(m), 541(w), 447(m). **1*-Gd** was obtained by Xe-lamp irradiation of compound **1-Gd** at room temperature for 60 min. For complex **1*-Gd** (%): calcd for $C_{18}H_{24}NO_{14}P_4Gd$ (759.51): C, 28.44; H, 3.16; N, 1.84. Found: C, 28.42; H, 3.17; N, 1.82. IR (KBr pellets, cm^{-1}): 1639(s), 1508(s), 1442(s), 1150(w), 1054(s), 910(s), 645(m), 549(s), 532(w), 452(s).

(H-4-spy)[Gd(H_2-HEDP)$_2$] (2-Gd)

(H-4-spy)[Gd(H_2-HEDP)$_2$] **(2-Gd).** The synthesis of compound **2- Gd** was used by the same method as compound **1-Dy** but using Gd_2O_3 (0.045 g, 0.10 mmol). Yield: ca. 41% based on Gd_2O_3. Elemental analysis for **2-Gd** (%): calcd for $C_{17}H_{24}NO_{14}P_4Gd$ (747.5): C, 27.29; H, 3.21; N, 1.87. Found: C, 27.31; H, 3.24; N, 1.88. IR (KBr pellets, cm-1): 1620(s), 1505(s), 1449(s), 1363(m), 1148(m), 1066(w), 972(m), 917(m), 814(s),

705(m), 651(s), 544(w), 449(m). **2*-Gd** was obtained by Xe-lamp irradiation of compound **2-Gd** at room temperature for 60 min. For complex **2*-Gd** (%): calcd for $C_{17}H_{24}NO_{14}P_4Gd$ (747.5): C, 27.29; H, 3.21; N, 1.87. Found: C, 27.30; H, 3.24; N, 1.88. IR (KBr pellets, cm-1): 1635(s), 1505(s), 1449(s), 1363(m), 1141(m), 1066(w), 972(s), 917(m), 814(s), 705(m), 651(s), 544(w), 451(m).

(H-4-Cl-4spy)[Gd(H_2-HEDP)$_2$] (3-Gd)

(H-4-Cl-4spy)[Gd(H_2-HEDP)$_2$] **(3-Gd).** The synthesis of compound **3-Gd** was used by the same method as compound **1-Dy** but using Gd_2O_3 (0.045 g, 0.10 mmol). Yield: ca. 48% based on Gd_2O_3. Elemental analysis for **3-Gd** (%): calcd for $C_{17}H_{24}NO_{14}P_4GdCl$ (783.96): C, 26.02; H, 3.06; N, 1.79. Found: C, 25.84; H, 3.08; N, 1.83. IR (KBr pellets, cm^{-1}): 1641(s), 1491(m), 1142(s), 1060(w), 978(m), 910(w), 810(s), 737(m), 649(s), 543(m), 451(s), 433(m). **3*-Gd** was obtained by Xe-lamp irradiation of compound **3-Gd** at room temperature for 60 min. For complex **3*-Gd** (%): calcd for $C_{17}H_{24}NO_{14}P_4GdCl$ (783.96): C, 26.02; H, 3.06; N, 1.79. Found: C, 25.84; H, 3.08; N, 1.83. IR (KBr pellets, cm^{-1}): 1625(s), 1502(m), 1403(s), 1142(s), 1060(w), 974(m), 915(w), 810(s), 645(s), 543(m), 451(m), 433(m).

X-ray Crystallography

The single-crystal XRD data of **1-Dy**, **2-Dy** and **3-Dy** were collected on a Rigaku XtaLAB Synergy R, DW system, HyPix diffractometer with Mo-Kα radiation. The Olex2 software was used to solve the structures.[1] Detailed crystallographic data for complexes **1-Dy**, **2-Dy** and **3-Dy** was summarized in Tables S1, and the selected bond lengths and angles were listed in Table S2, S3 and S4. Full crystallographic data have been deposited with the CCDC-2523763 for **1-Dy**, 2528876 for **2-Dy** and 2523764 for **3-Dy**.

References

1. O. V. Dolomanov; L. J. Bourhis; R. J. Gildea; J. A. K. Howard; H. Puschmann. OLEX2: a complete structure solution, refinement and analysis program. *J. Appl. Crystallogr.* **2009**, *42*, 339-341.

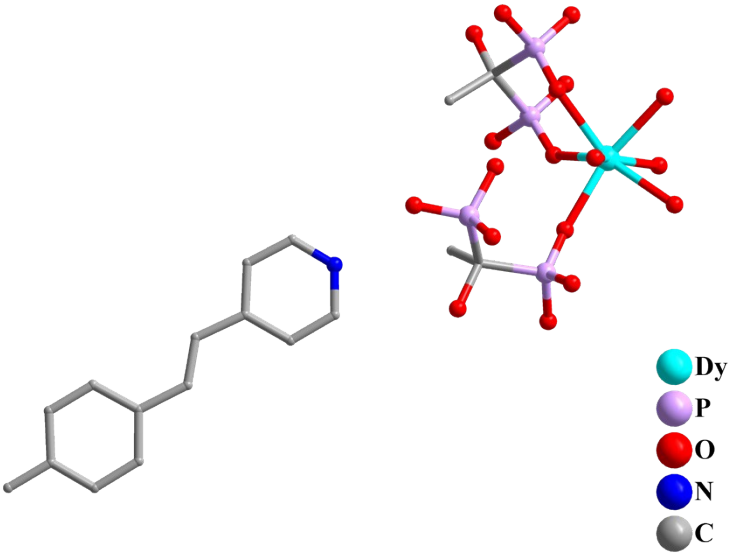

Fig. S1 The asymmetric unit of compound **1-Dy.**

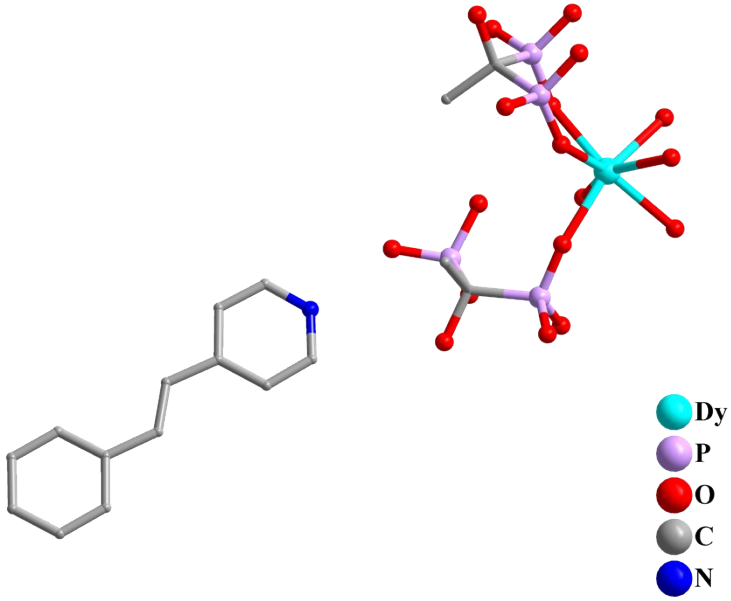

Fig. S2 The asymmetric unit of compound **2-Dy**.

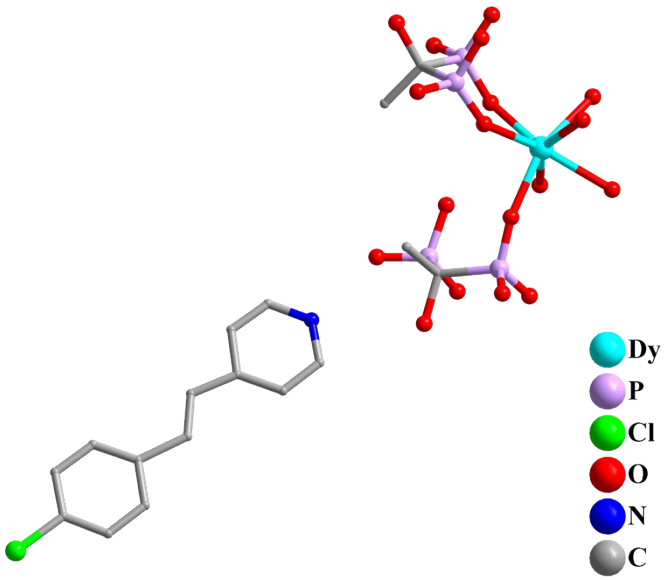

Fig. S3 The asymmetric unit of compound **3-Dy**.

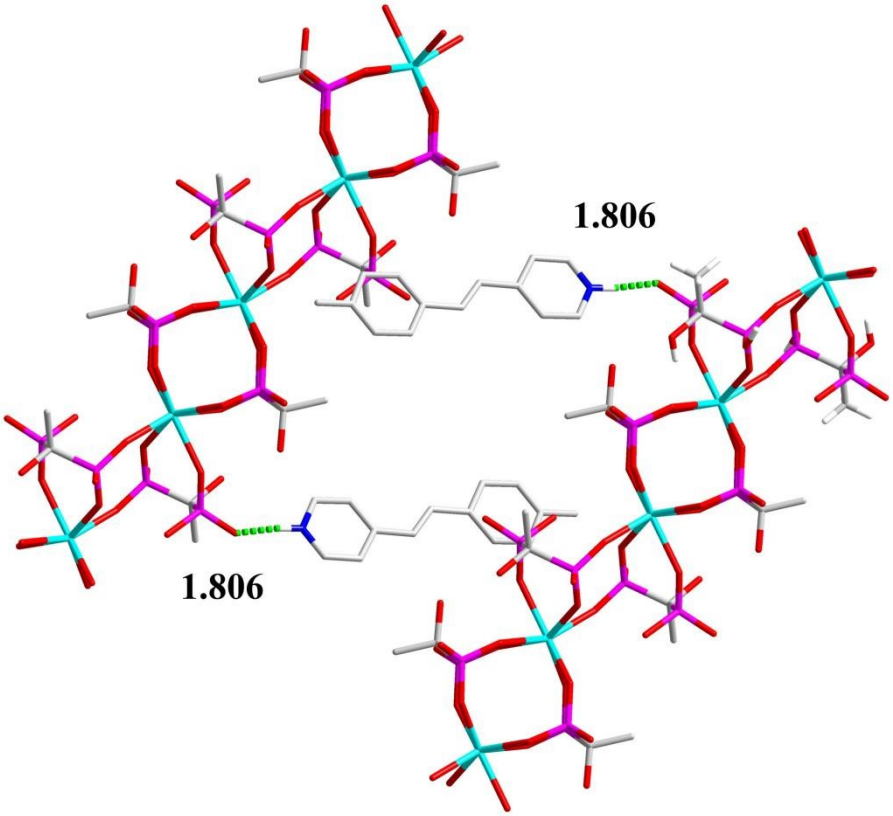

Fig. S4 The packing mode of **1-Dy** with H-bonds is shown as dashed lines.

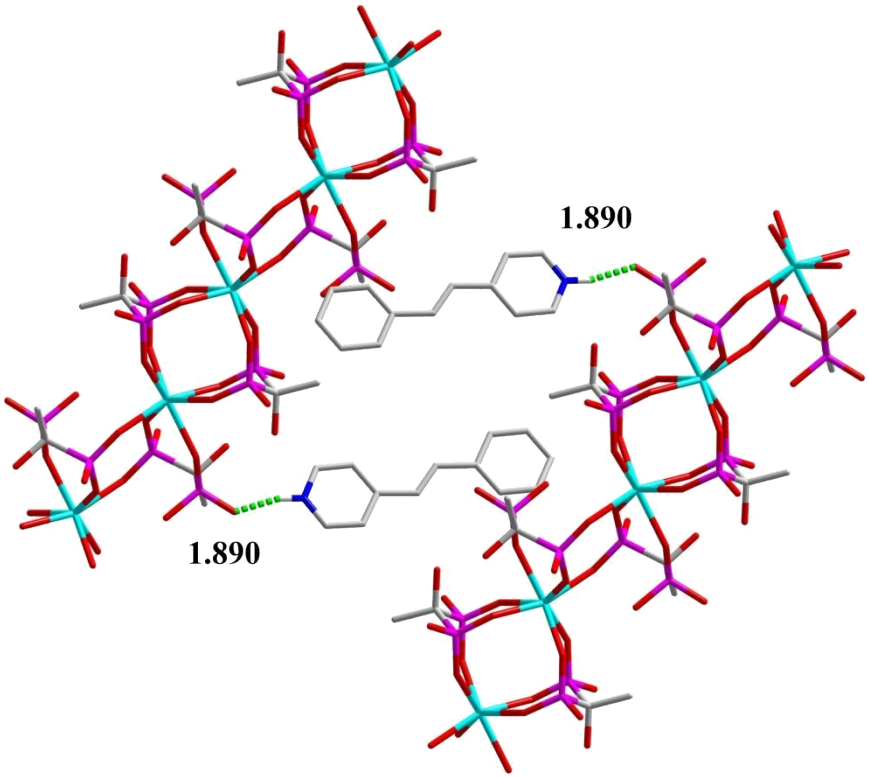

Fig. S5 The packing mode of **2-Dy** with H-bonds is shown as dashed lines.

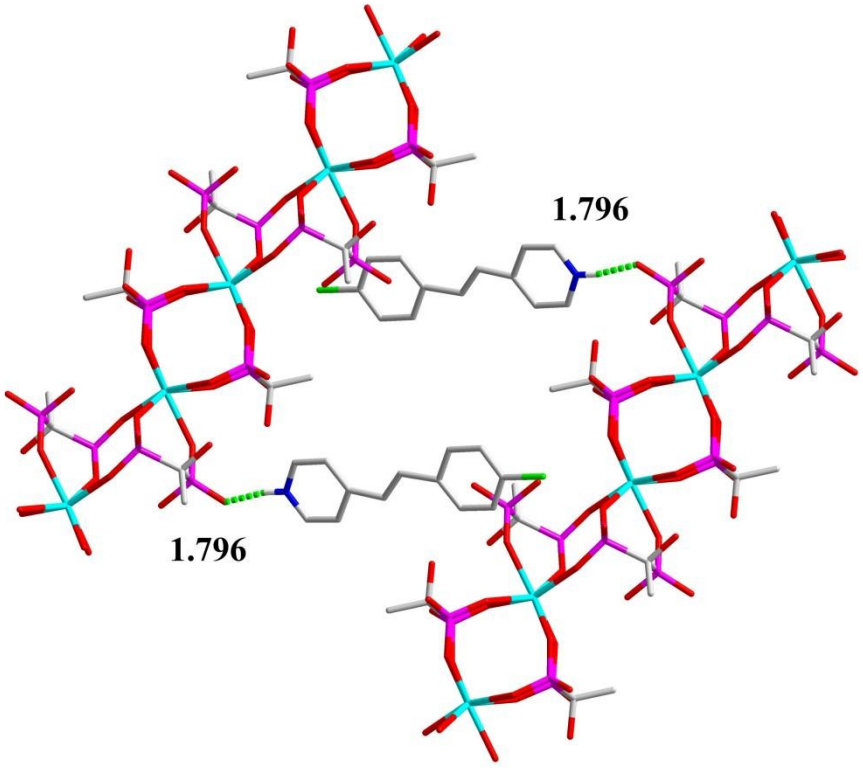

Fig. S6 The packing mode of **3-Dy** with H-bonds is shown as dashed lines.

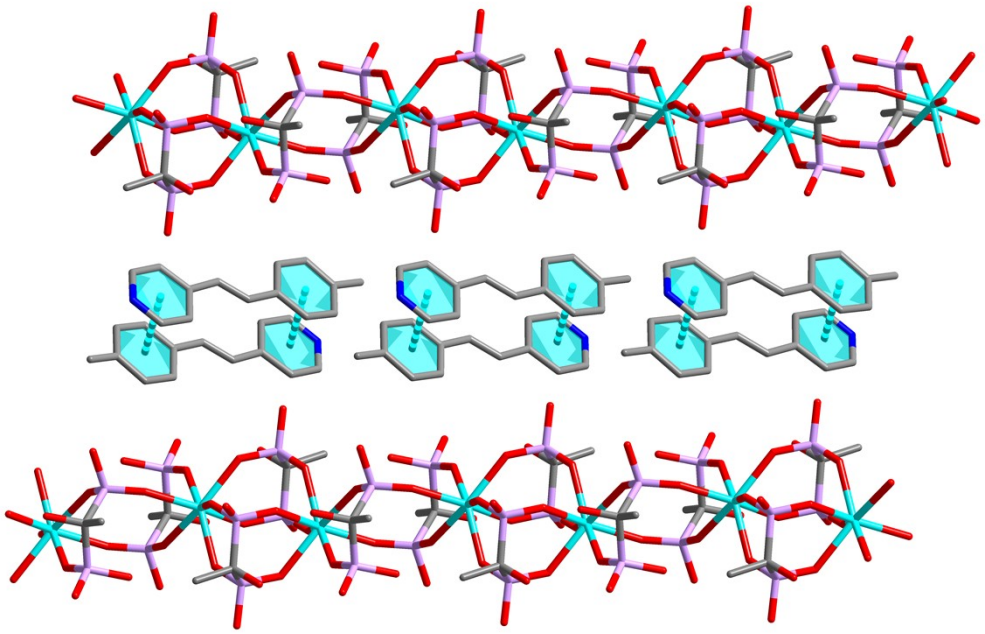

Fig. S7 The π-π stacking interaction between ligands in **1-Dy**.

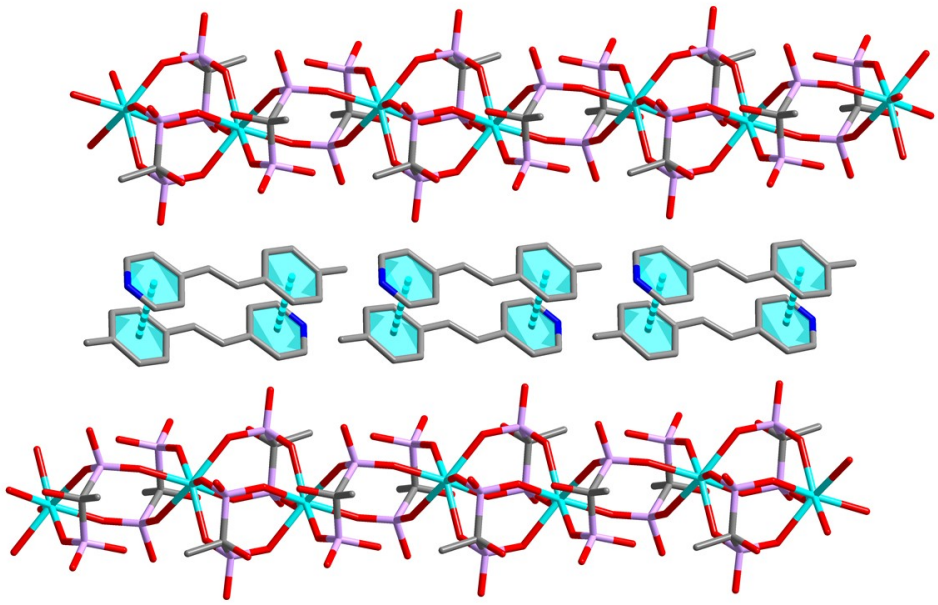

Fig. S8 The π-π stacking interaction between ligands in **2-Dy**.

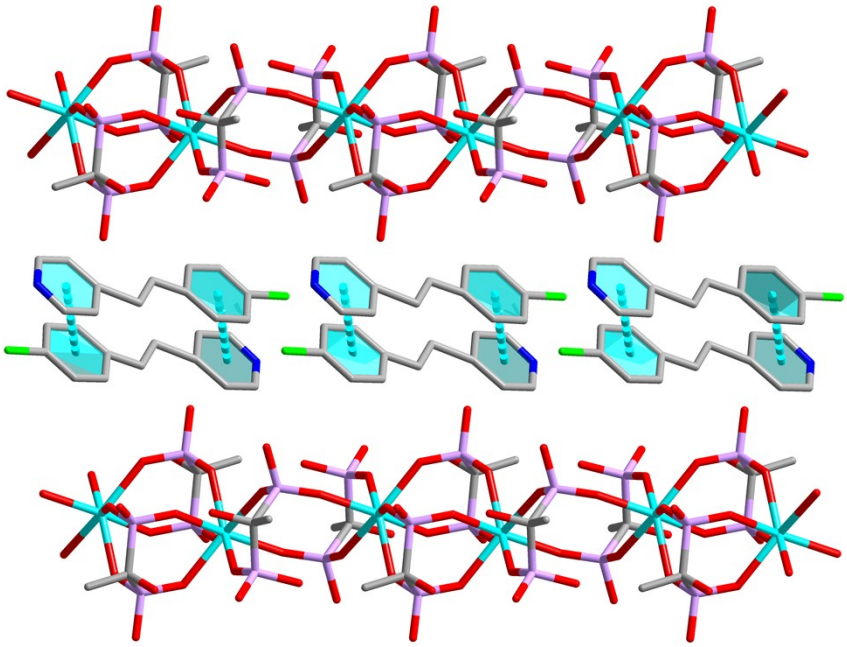

Fig. S9 The π-π stacking interaction between ligands in **3-Dy**.

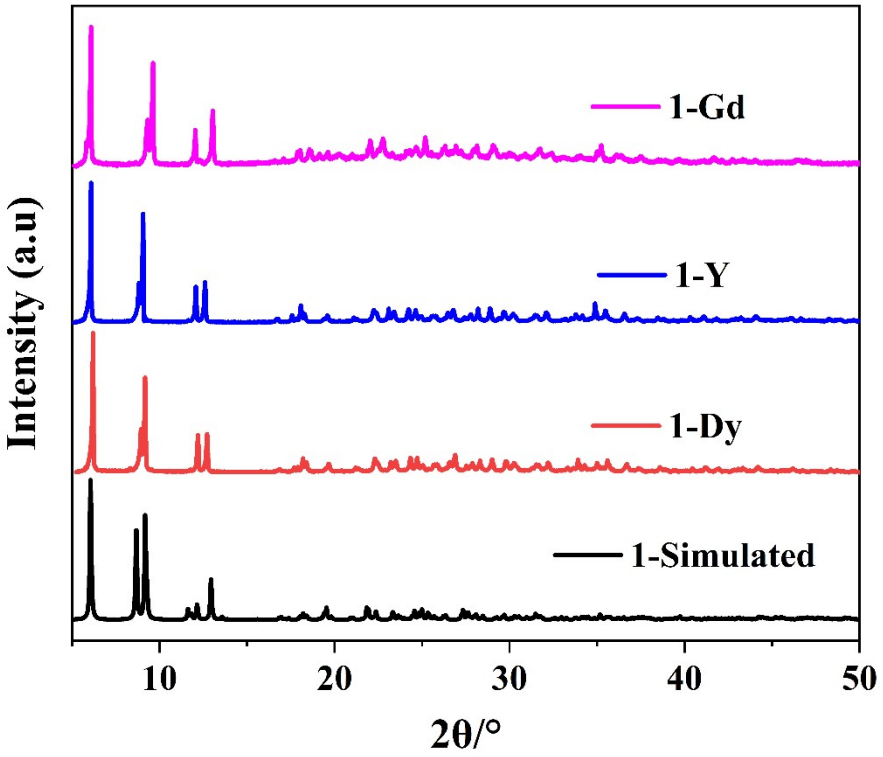

Fig. S10 PXRD patterns of simulated, experimental complexes **1-Dy**, **1-Y**, and **1-Gd**.

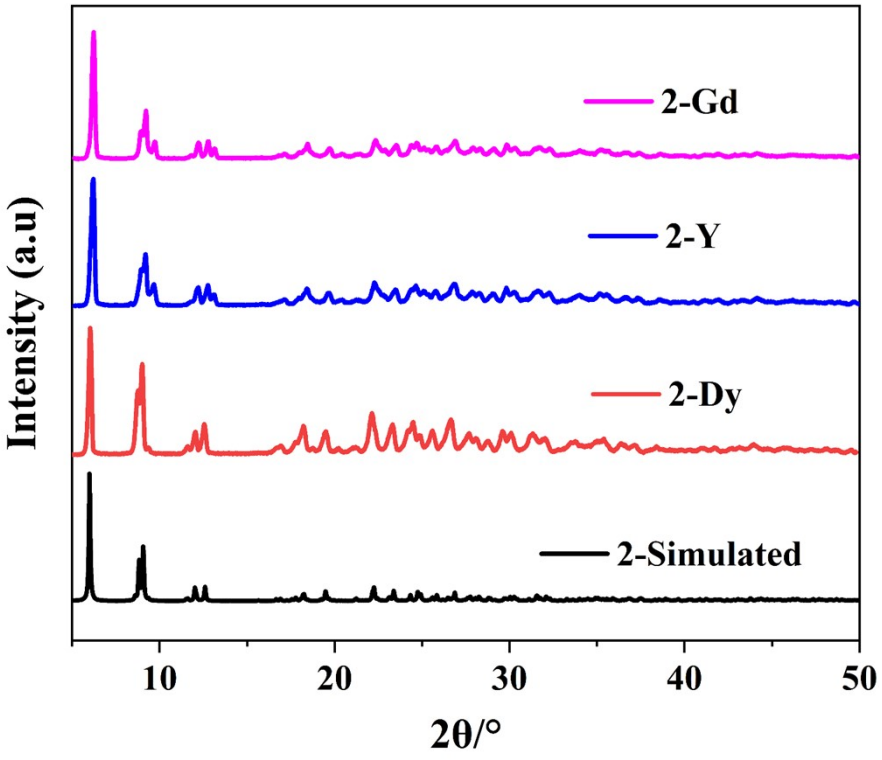

Fig. S11 PXRD patterns of simulated, experimental complexes **2-Dy**, **2-Y**, and **2-Gd**.

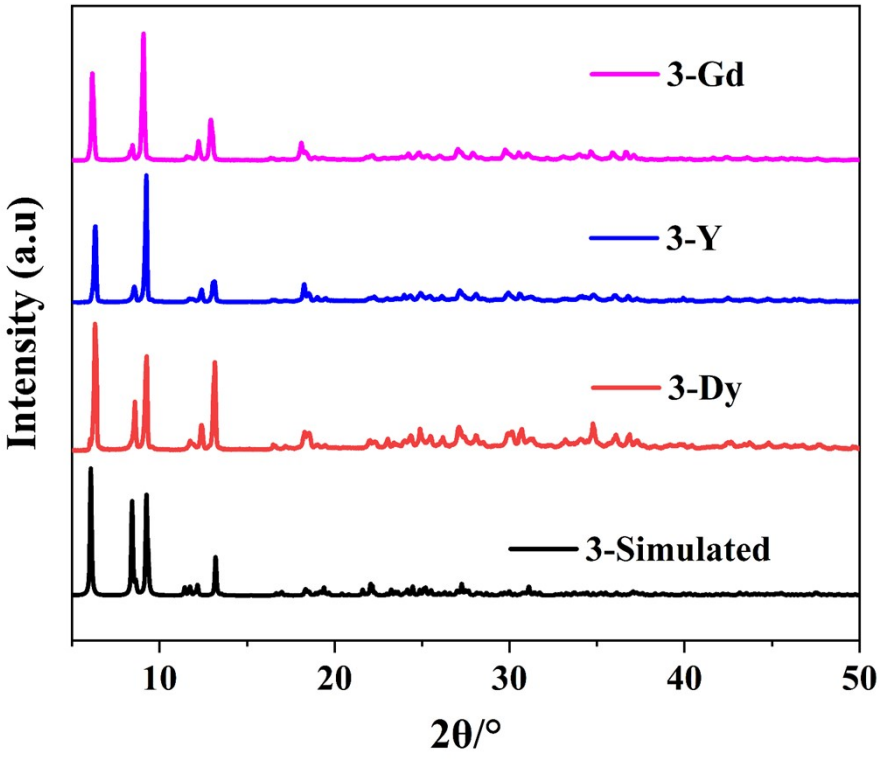

Fig. S12 PXRD patterns of simulated, experimental complexes **3-Dy**, **3-Y**, and **3-Gd**.

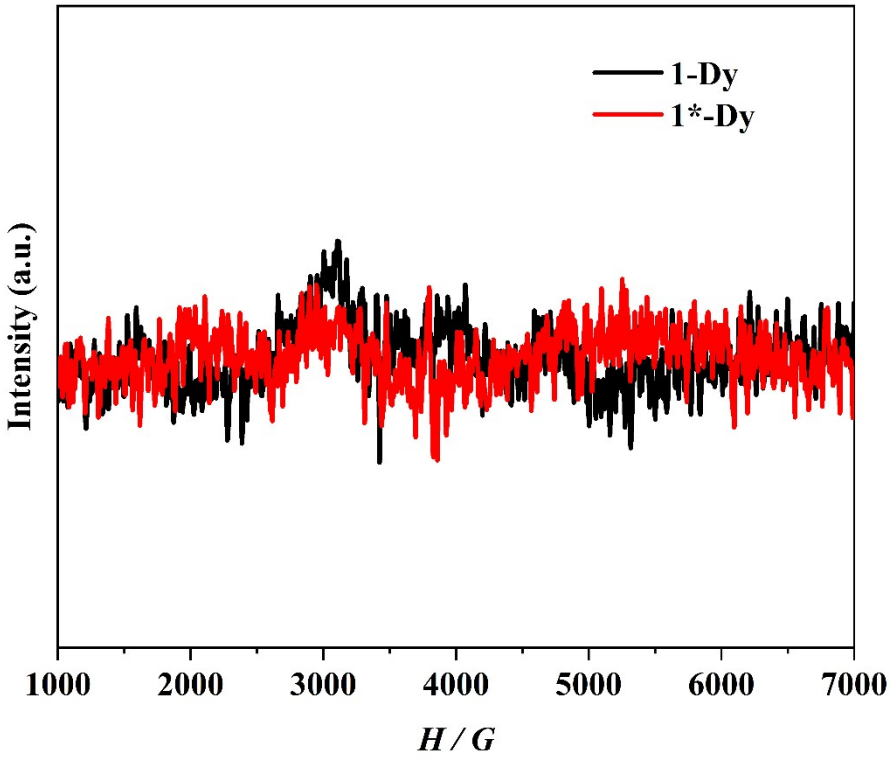

Fig. S13 Solid-state EPR spectra of **1-Dy** before and after light irradiation recorded at room temperature at a frequency of 9.54 GHz.

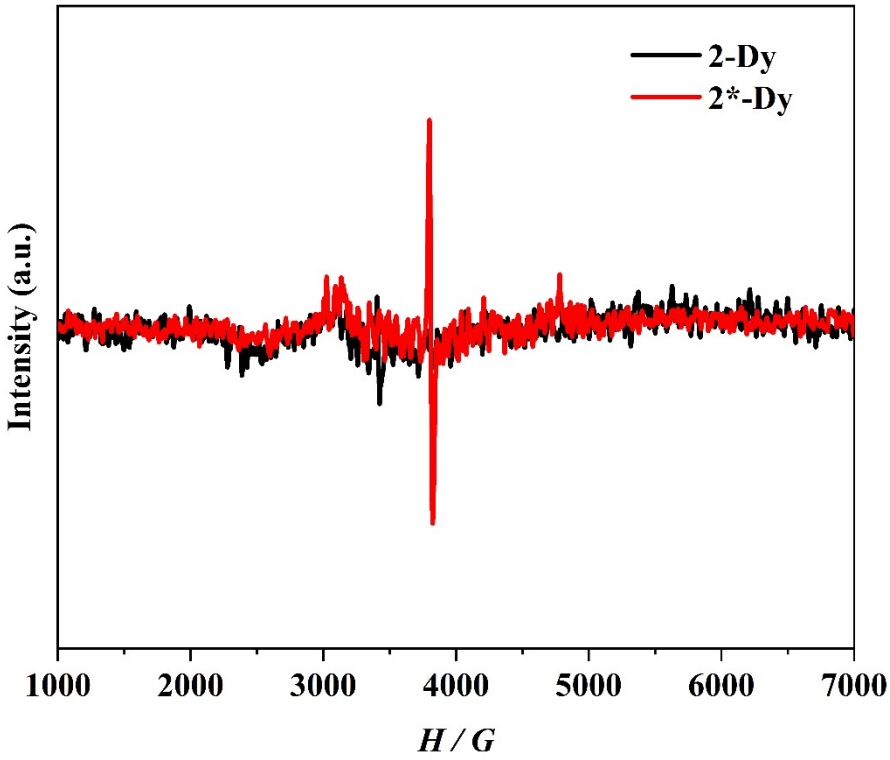

Fig. S14 Solid-state EPR spectra of **2-Dy** before and after light irradiation recorded at room temperature at a frequency of 9.54 GHz.

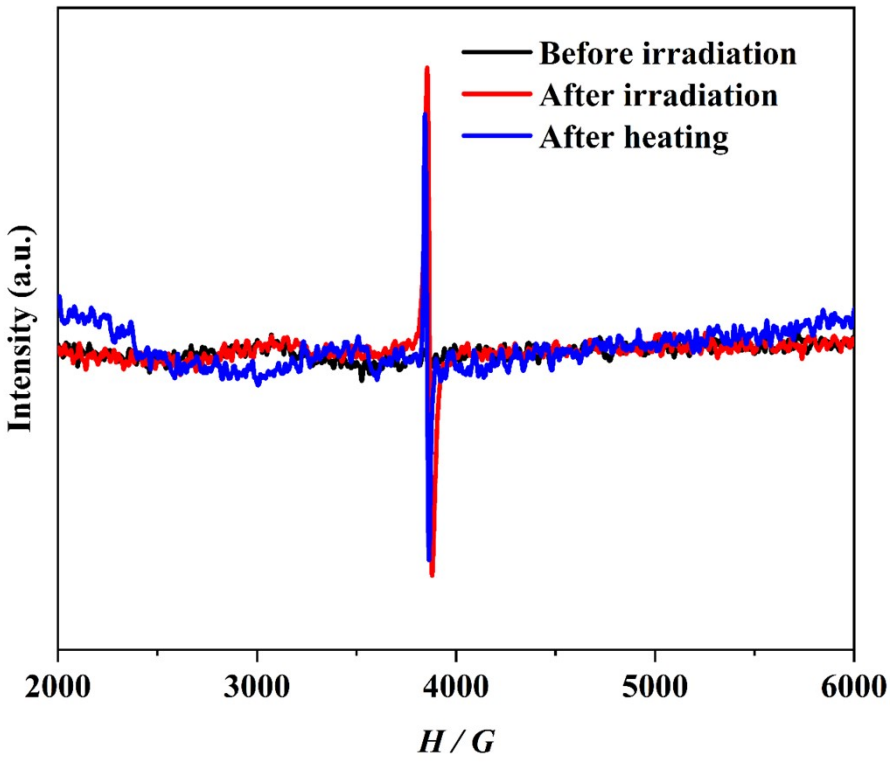

Fig. S15 Solid-state EPR spectra of **3-Dy** before and after light irradiation and after heating recorded at room temperature at a frequency of 9.54 GHz.

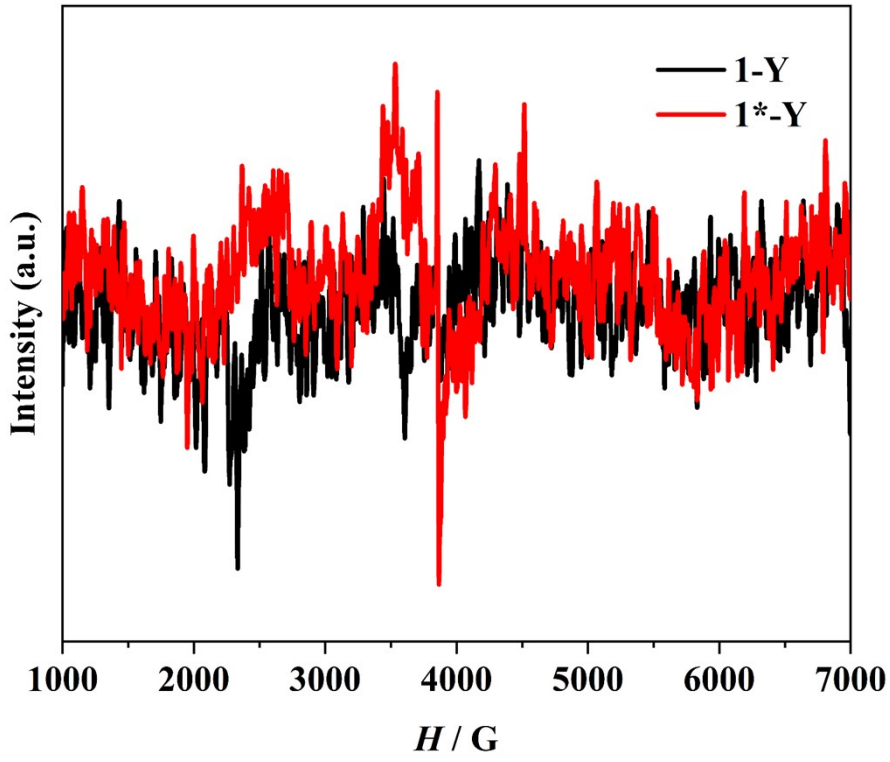

Fig. S16 Solid-state EPR spectra of **1-Y** before and after light irradiation recorded at room temperature at a frequency of 9.54 GHz.

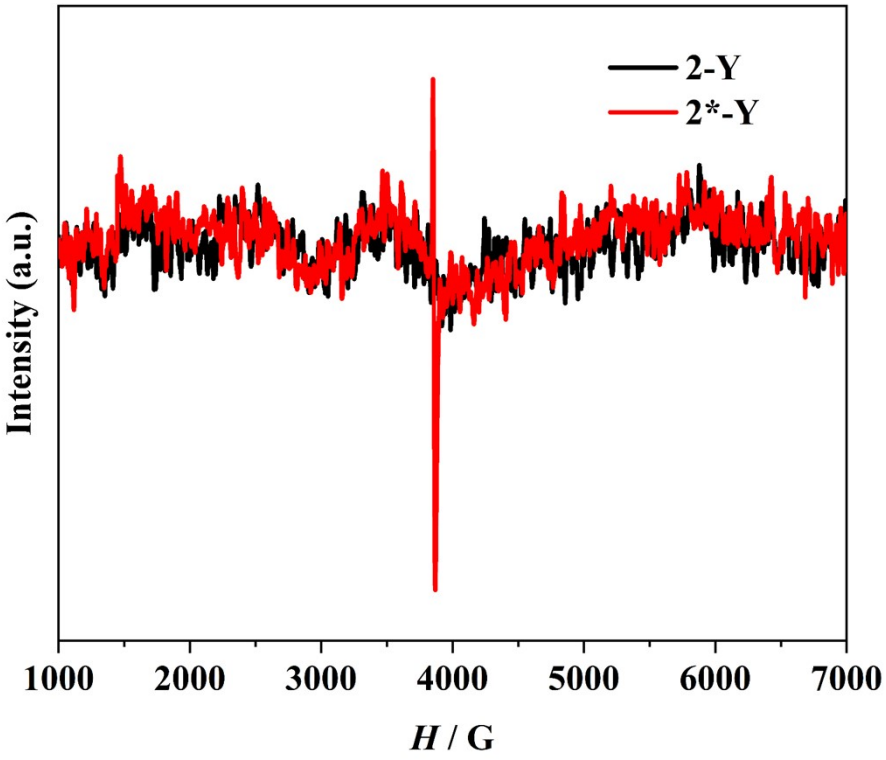

Fig. S17 Solid-state EPR spectra of **2-Y** before and after light irradiation recorded at room temperature at a frequency of 9.54 GHz.

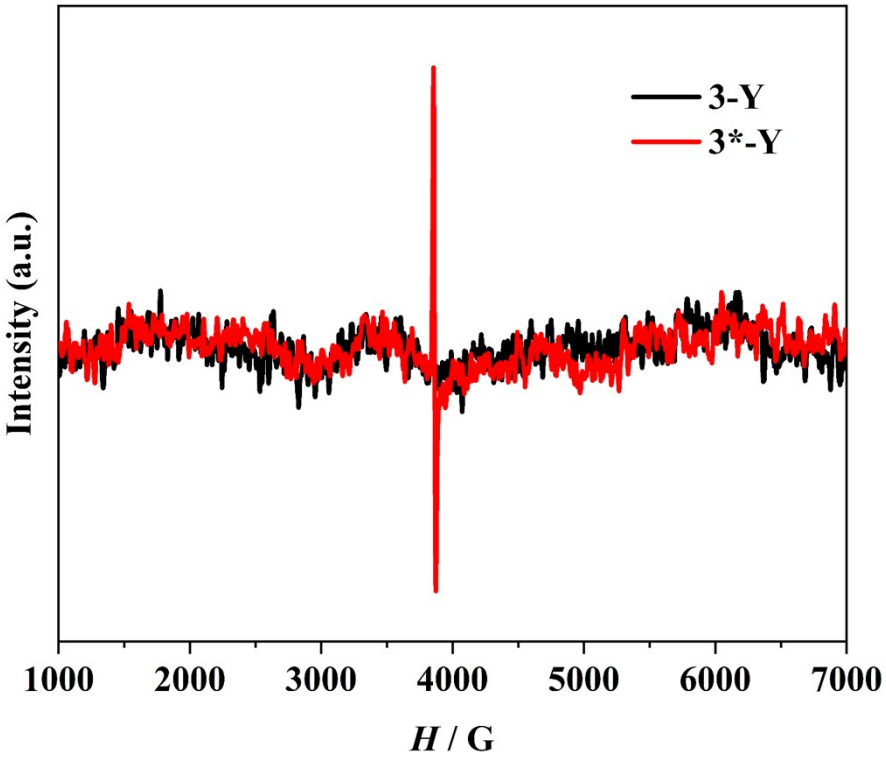

Fig. S18 Solid-state EPR spectra of **3-Y** before and after light irradiation recorded at room temperature at a frequency of 9.54 GHz.

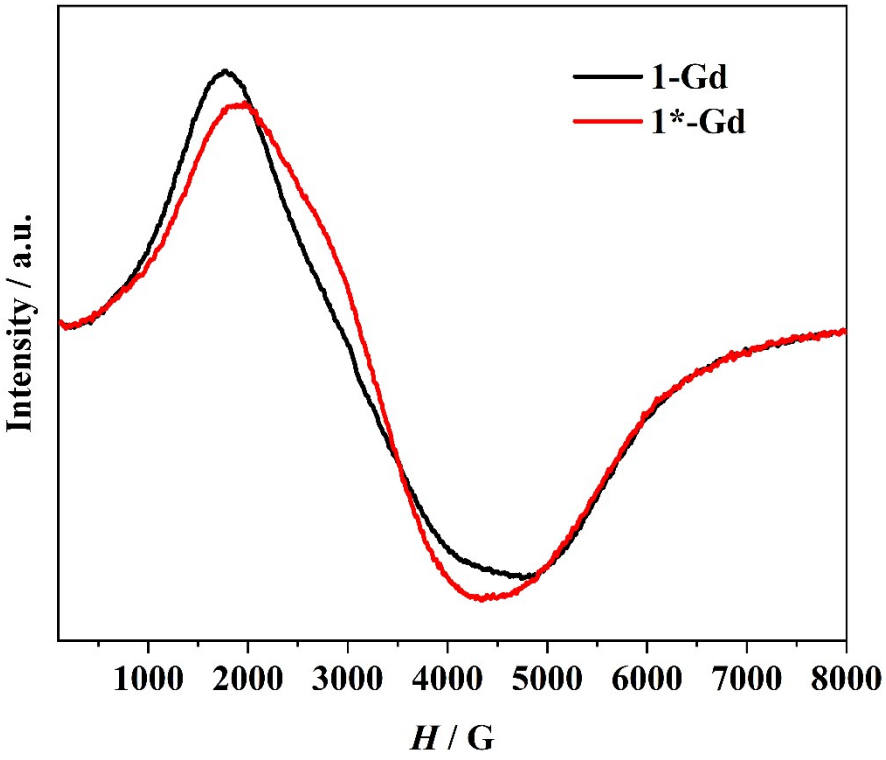

Fig. S19 Solid-state EPR spectra of **1-Gd** before and after light irradiation recorded at room temperature at a frequency of 9.54 GHz.

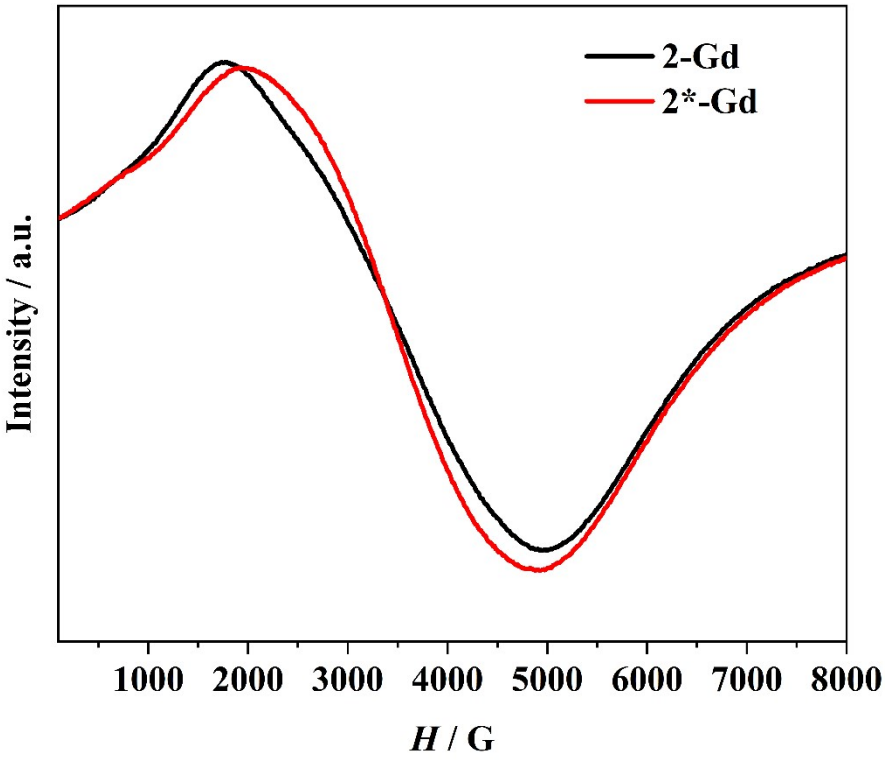

Fig. S20 Solid-state EPR spectra of **2-Gd** before and after light irradiation recorded at room temperature at a frequency of 9.54 GHz.

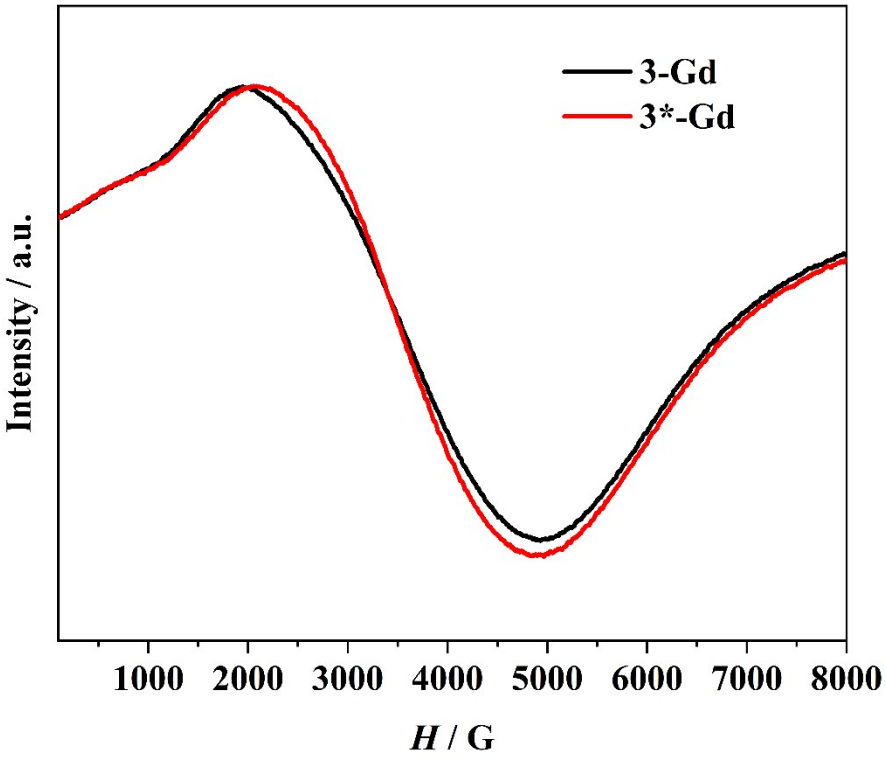

Fig. S21 Solid-state EPR spectra of **3-Gd** before and after light irradiation recorded at room temperature at a frequency of 9.54 GHz.

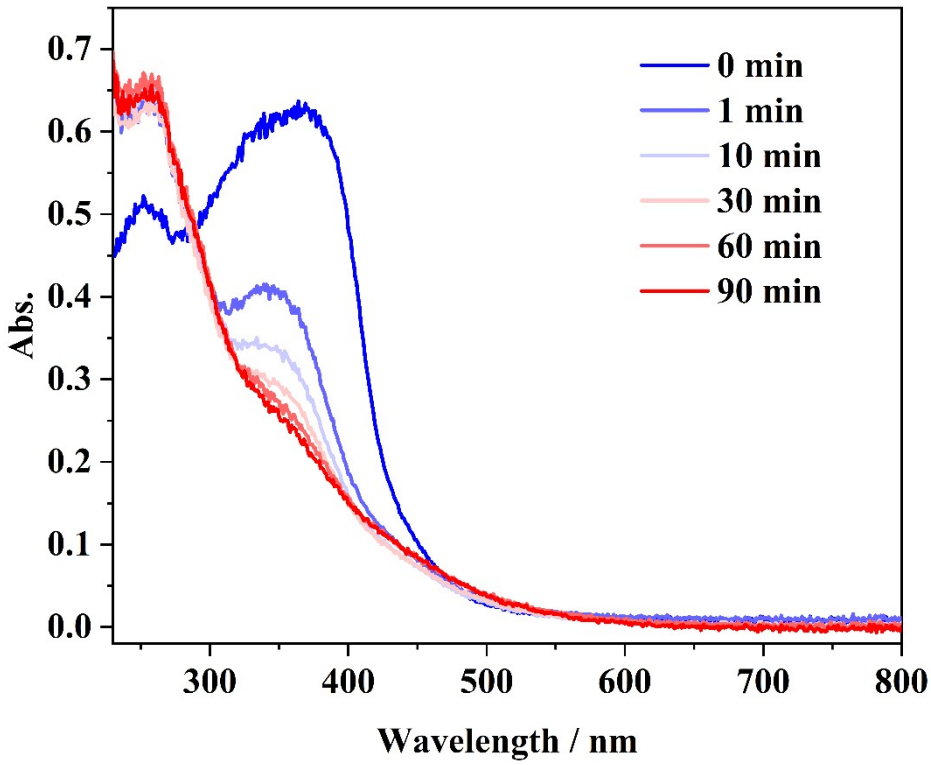

Fig. S22 Solid-state UV–vis absorption spectra of **1-Gd** at different irradiation time.

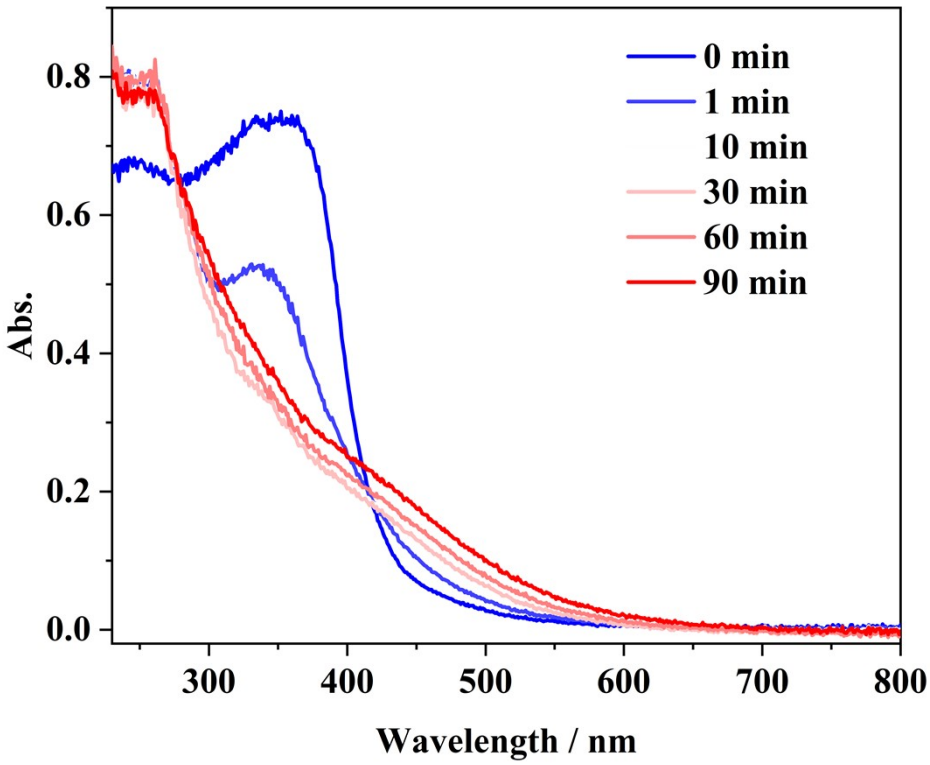

Fig. S23 Solid-state UV–vis absorption spectra of **2-Gd** at different irradiation time.

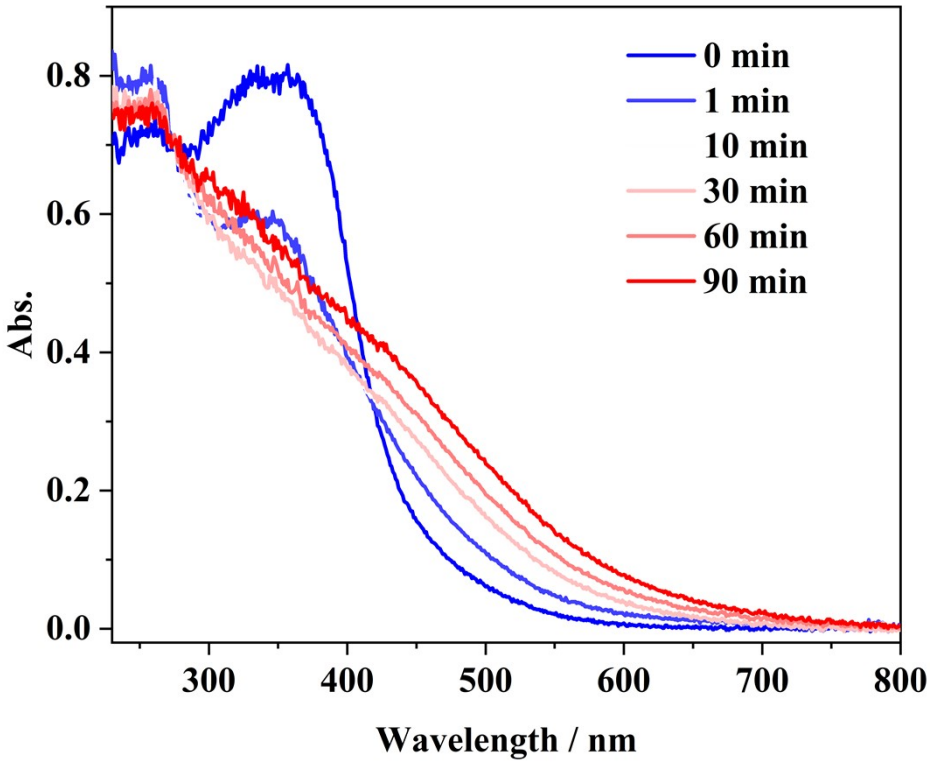

Fig. S24 Solid-state UV–vis absorption spectra of **3-Gd** at different irradiation time.

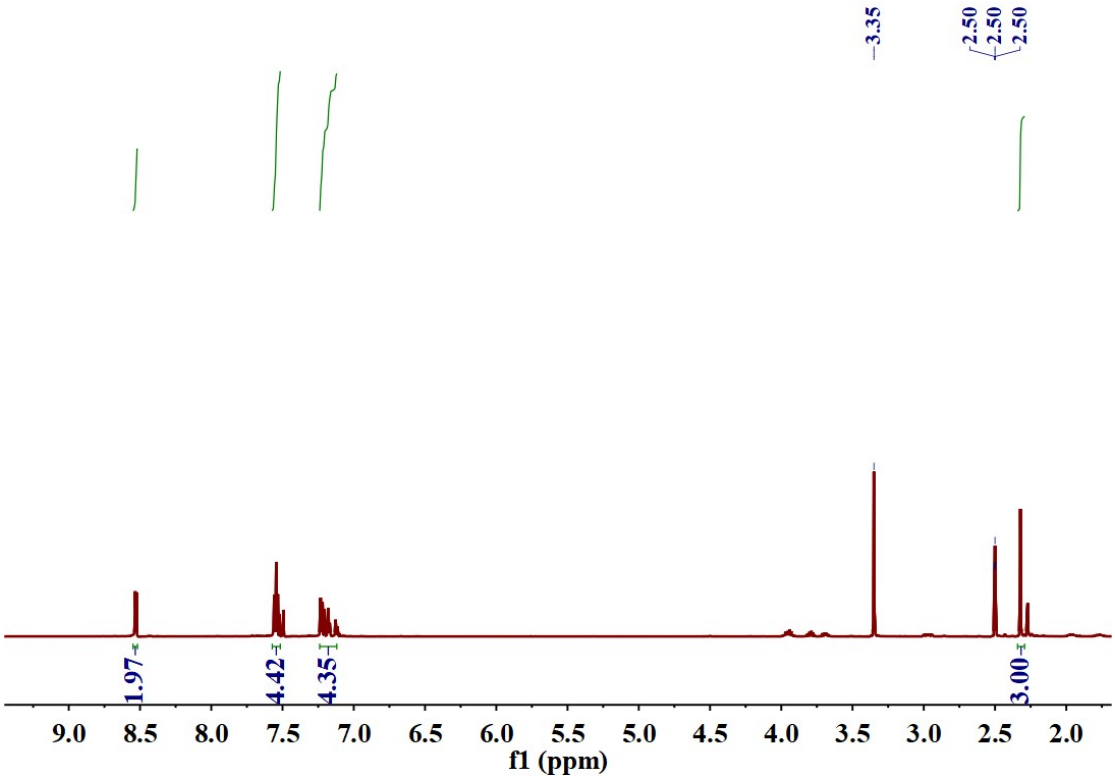

Fig. S25 ^{1}H NMR (400 MHz, DMSO-d_6, room temperature) spectra before and after irradiation of Me-4-arylethene.

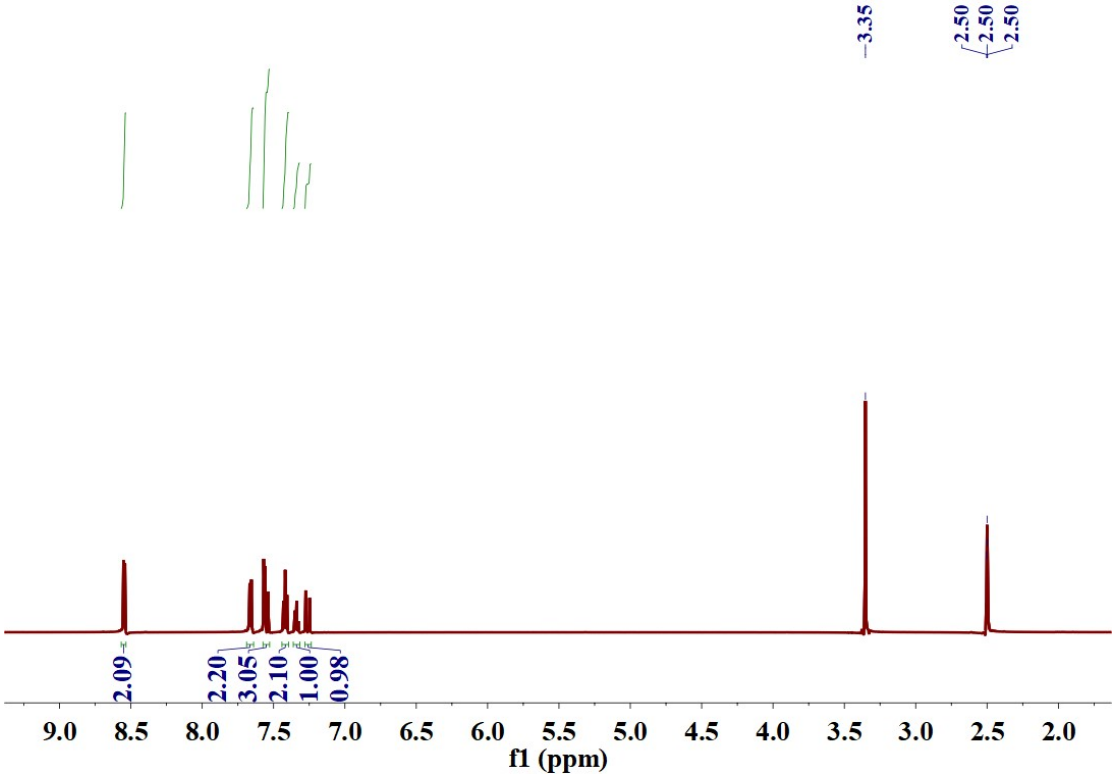

Fig. S26 ^{1}H NMR (400 MHz, DMSO-d_6, room temperature) spectra before and after irradiation of H-4-arylethene.

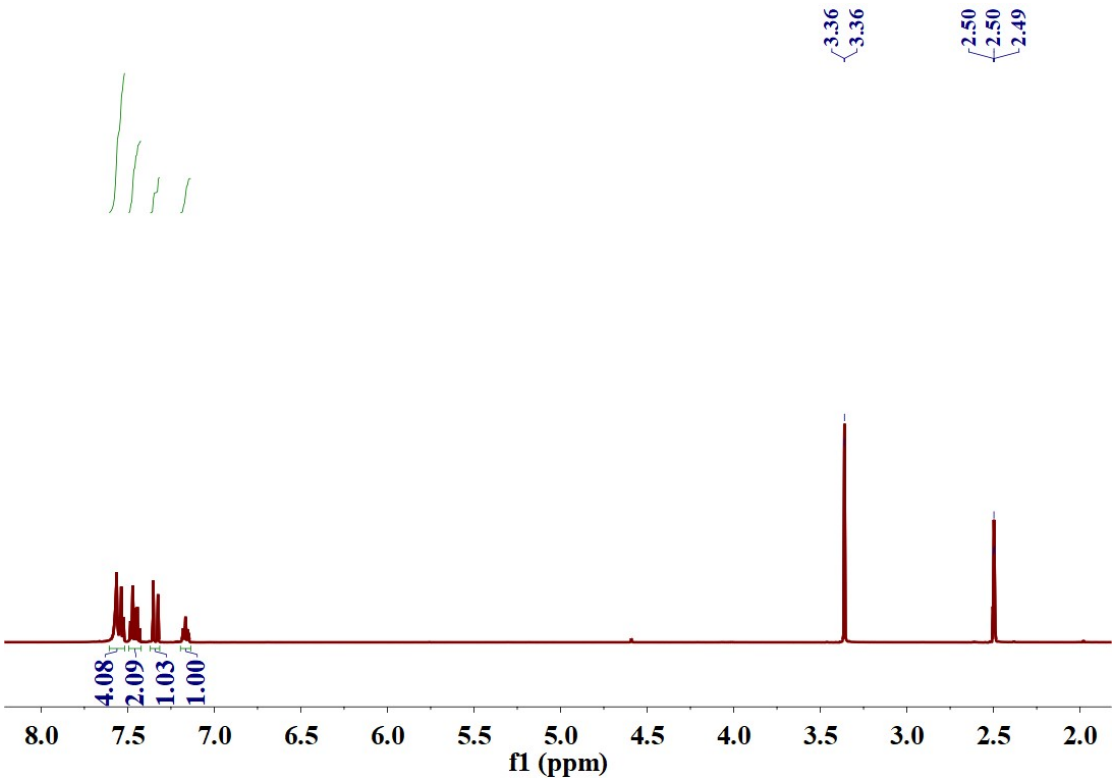

Fig. S27 ^{1}H NMR (400 MHz, DMSO-d_6, room temperature) spectra before and after irradiation of Cl-4-arylethene.

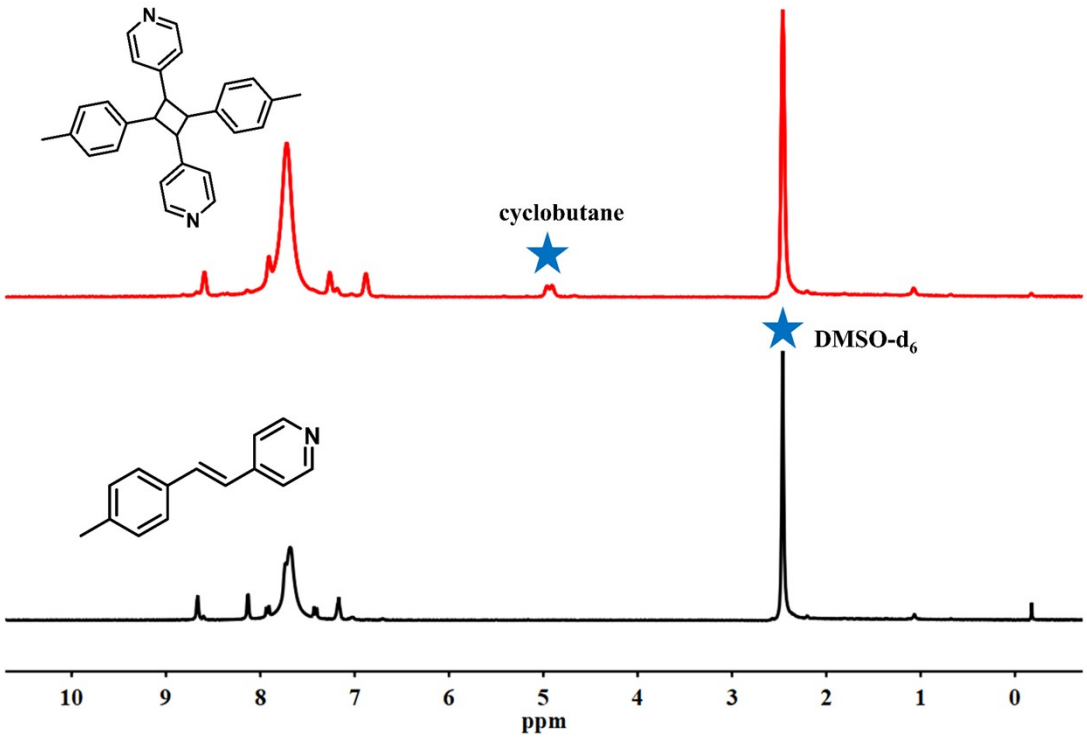

Fig. S28 ^{1}H NMR (400 MHz, DMSO-d_6, room temperature) spectra before and after irradiation of **1-Dy**.

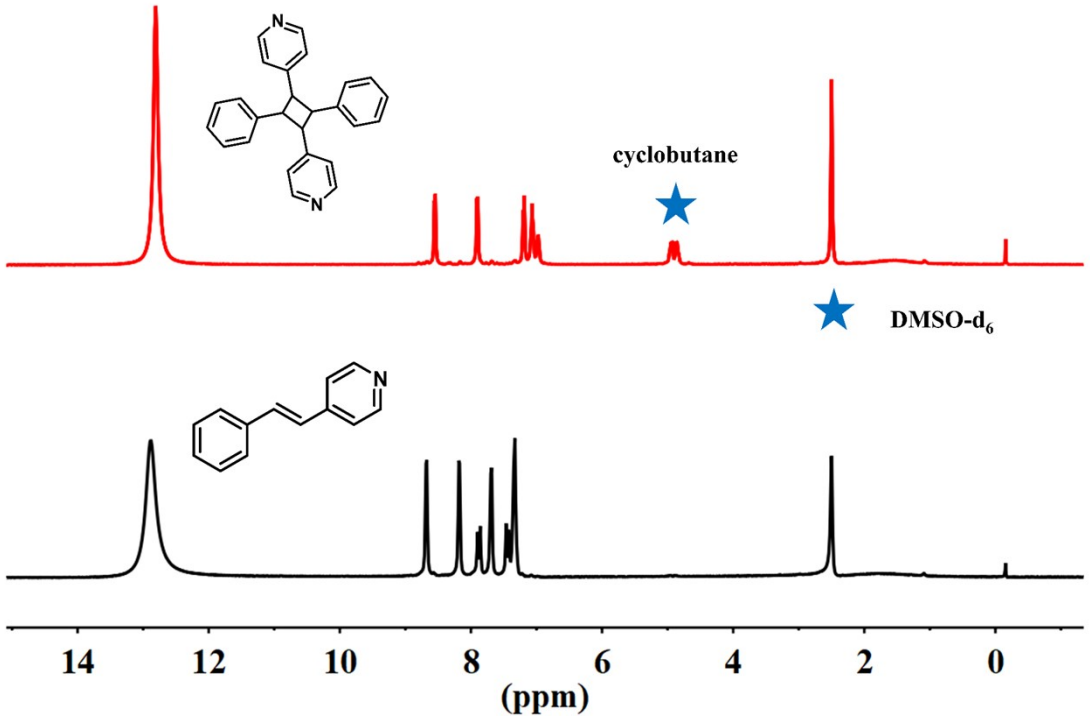

Fig. S29 ^{1}H NMR (400 MHz, DMSO-d_6, room temperature) spectra before and after irradiation of **2-Dy**.

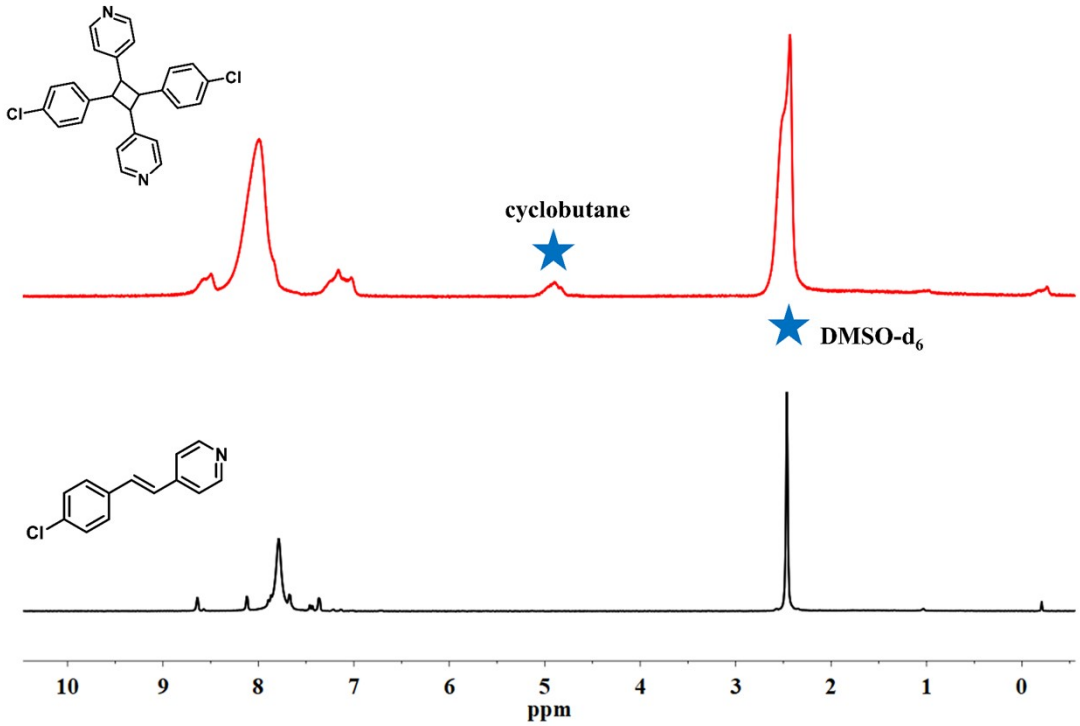

Fig. S30 ^{1}H NMR (400 MHz, DMSO-d_6, room temperature) spectra before and after irradiation of **3-Dy**.

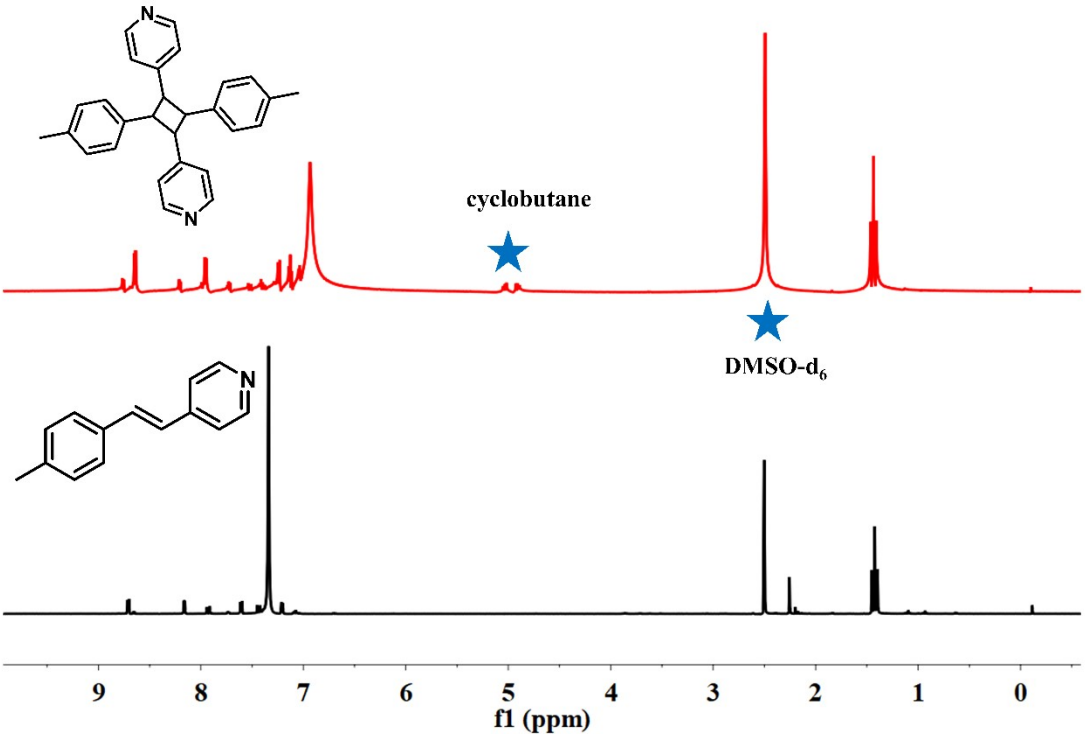

Fig. S31 ^{1}H NMR (400 MHz, DMSO-d_6, room temperature) spectra before and after irradiation of **1-Y**.

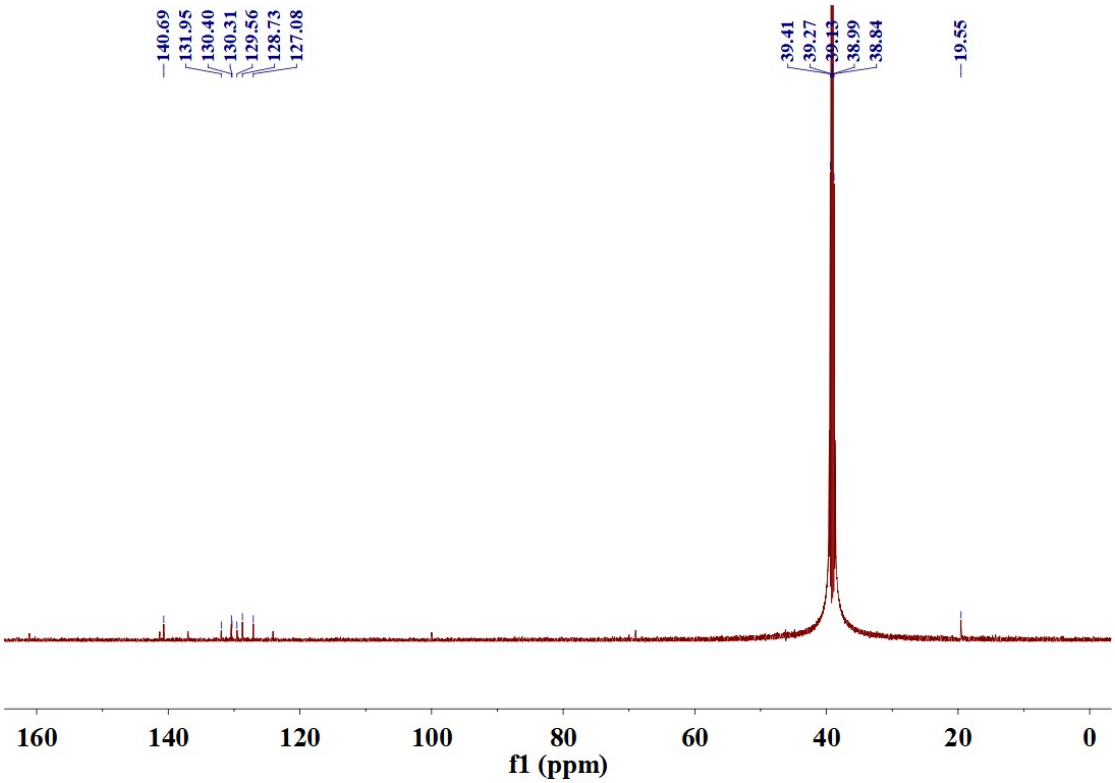

Fig. S32 ^{13}C NMR (400 MHz, DMSO-d_6, room temperature) spectra before and after irradiation of **1-Y**.

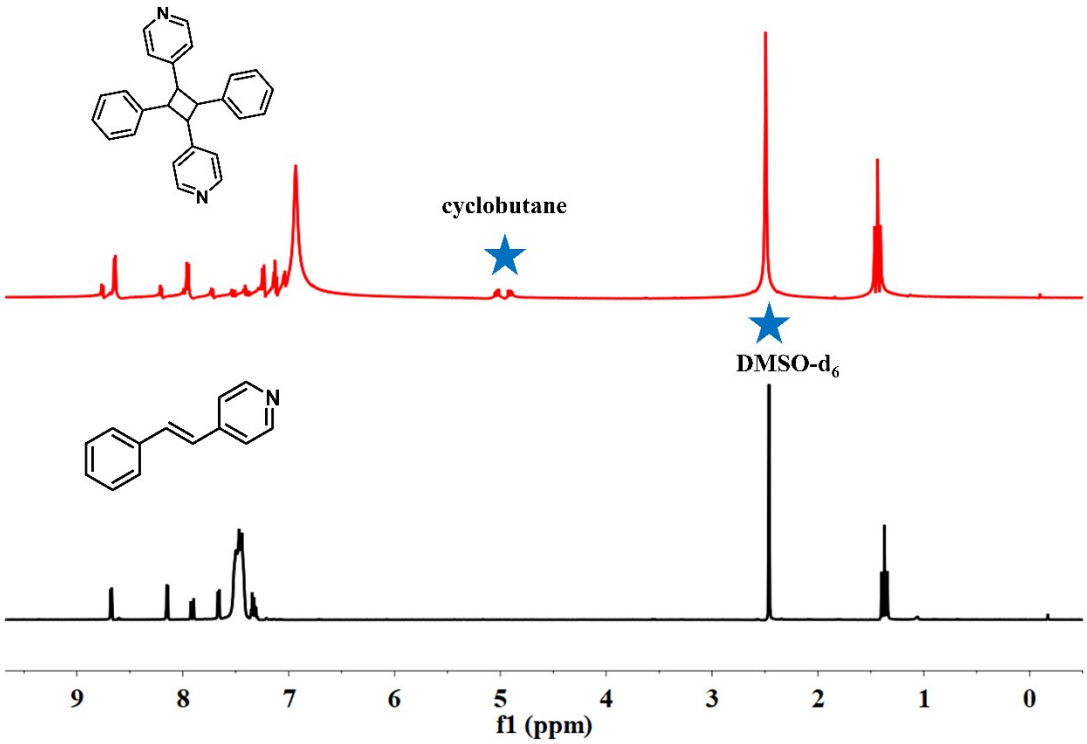

Fig. S33 ^{1}H NMR (400 MHz, DMSO-d_6, room temperature) spectra before and after irradiation of **2-Y**.

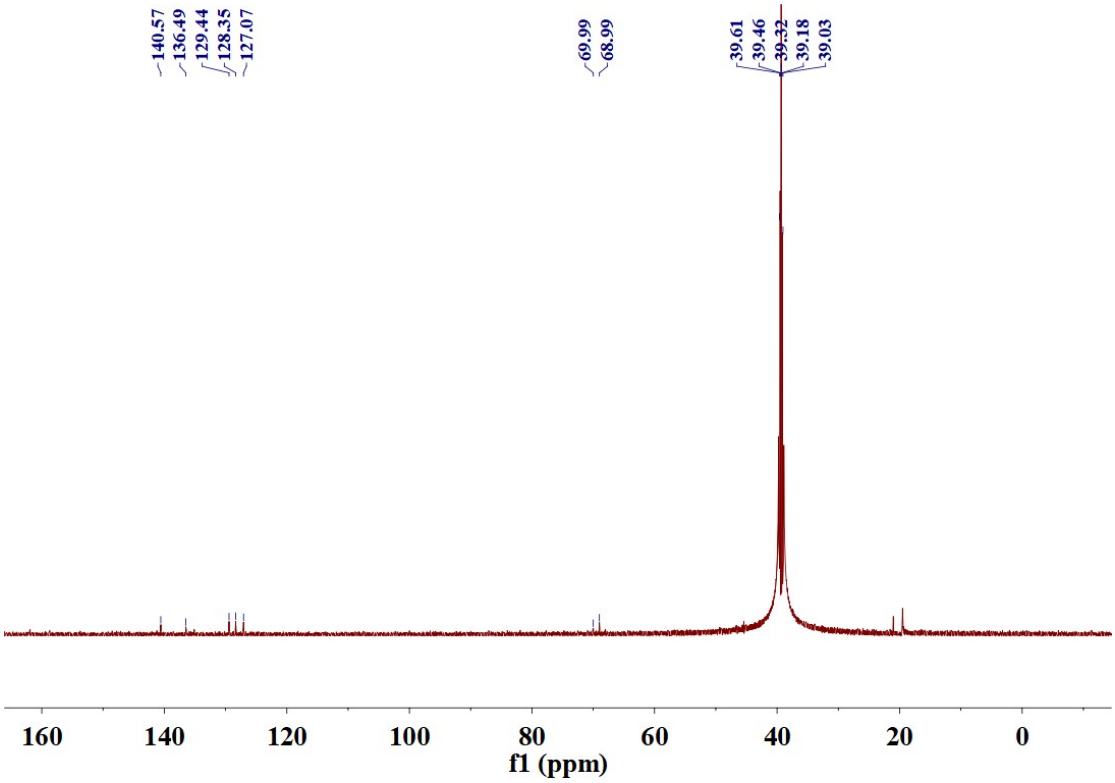

Fig. S34 ^{13}C NMR (400 MHz, DMSO-d_6, room temperature) spectra before and after irradiation of **2-Y**.

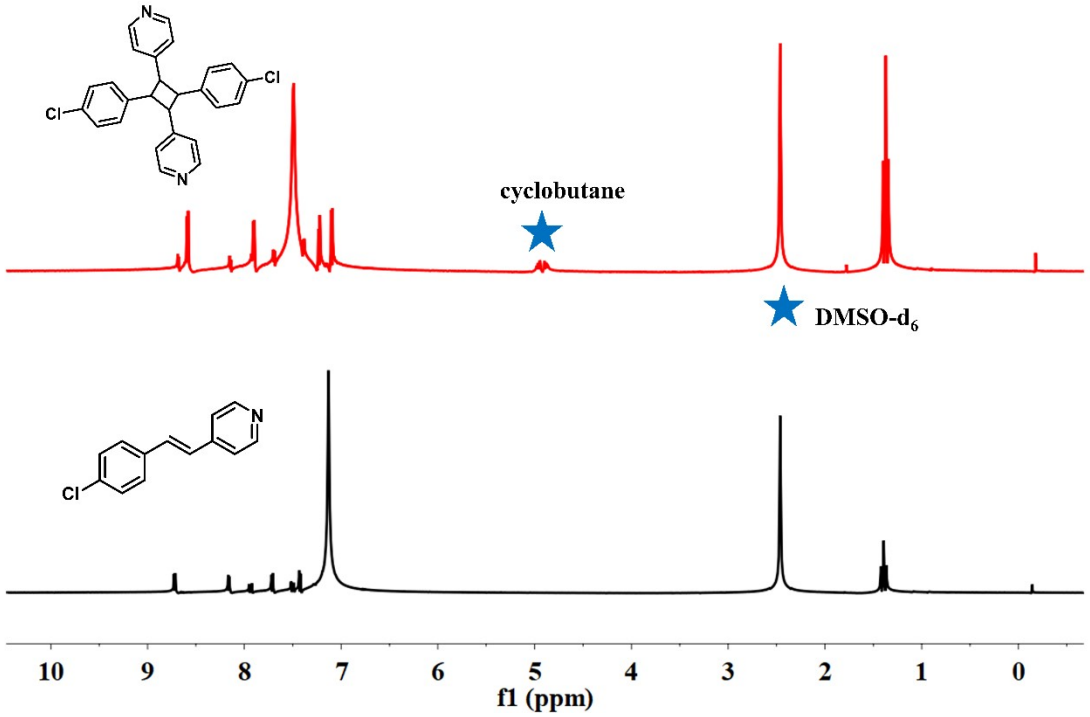

Fig. S35 ^{1}H NMR (400 MHz, DMSO-d_6, room temperature) spectra before and after irradiation of **3-Y**.

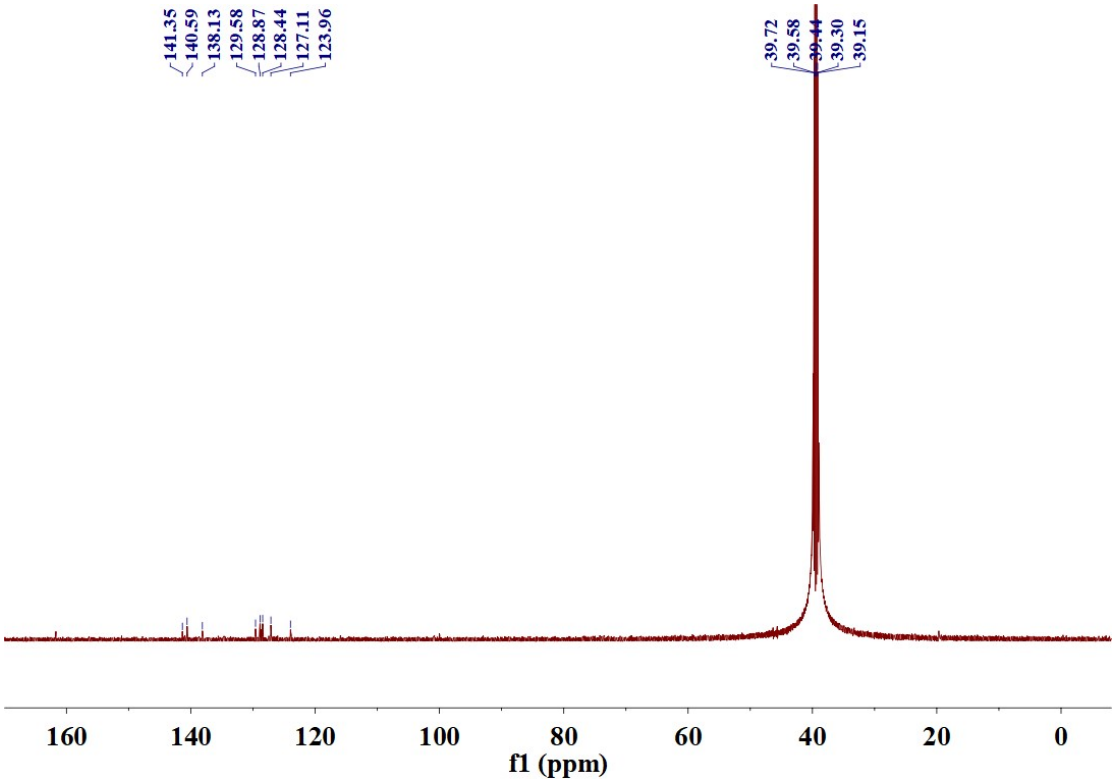

Fig. S36 ^{13}C NMR (400 MHz, DMSO-d_6, room temperature) spectra before and after irradiation of **3-Y**.

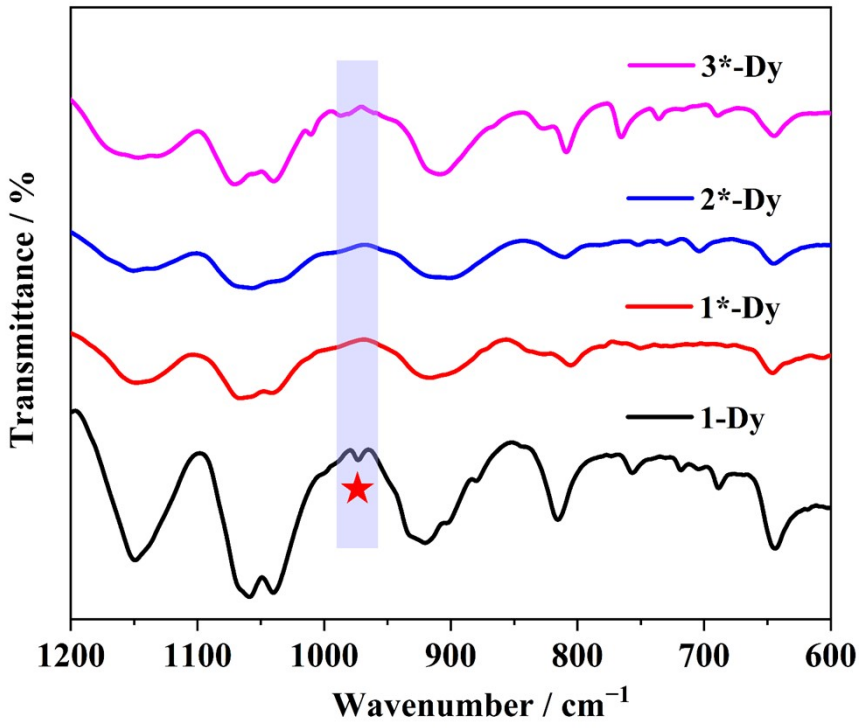

Fig. S37 Room-temperature IR spectra of the irradiated samples with different substituents in the Dy series recorded using a diamond ATR probe.

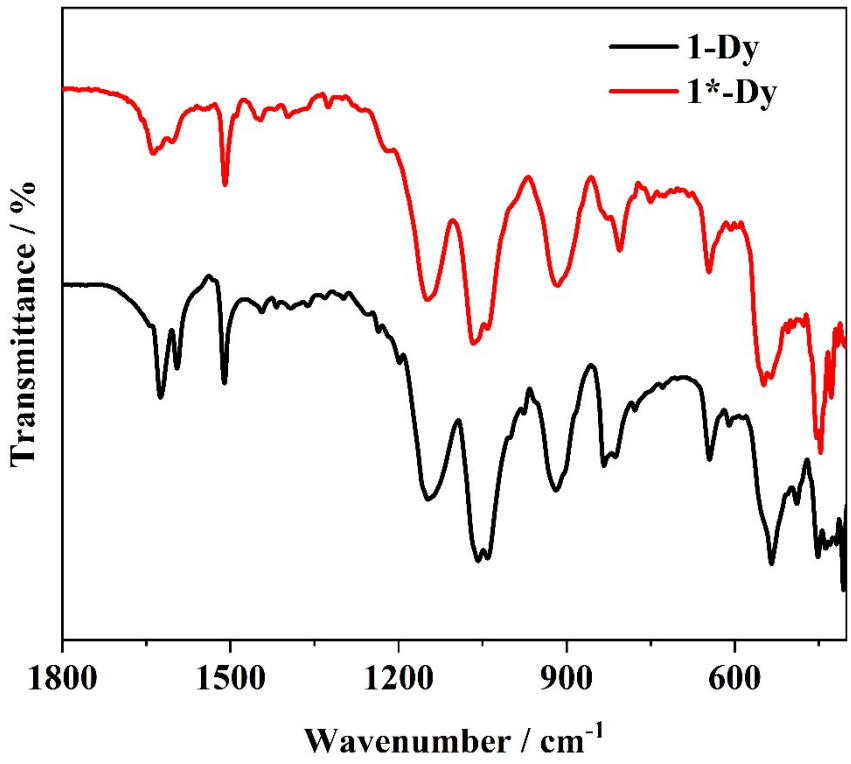

Fig. S38 Room-temperature IR spectra of **1-Dy** and the corresponding irradiated sample **1*-Dy** recorded using a diamond ATR probe.

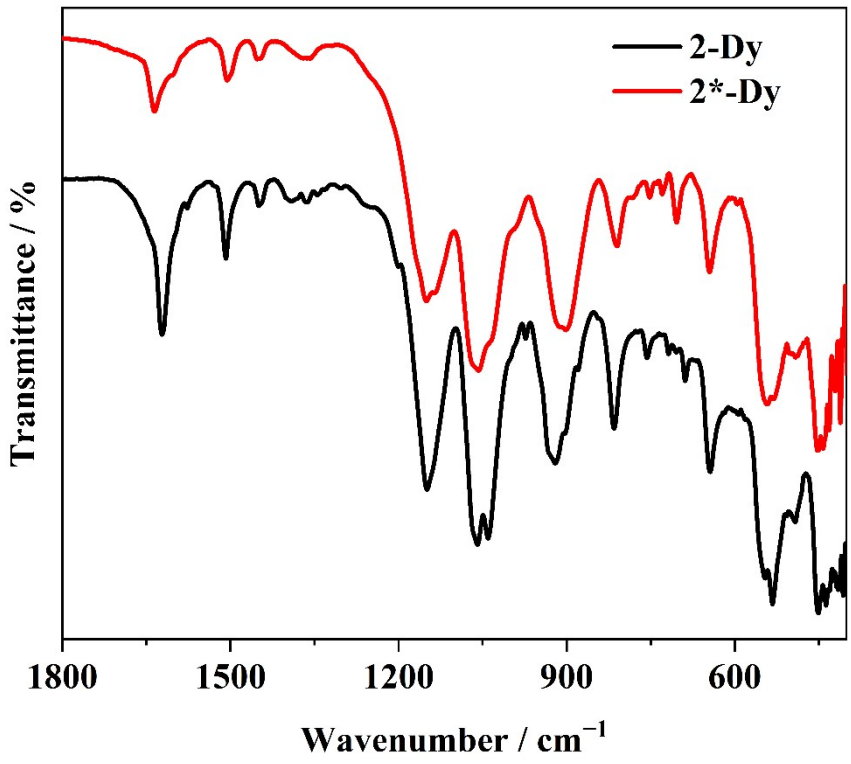

Fig. S39 Room-temperature IR spectra of **2-Dy** and the corresponding irradiated sample **2*-Dy** recorded using a diamond ATR probe.

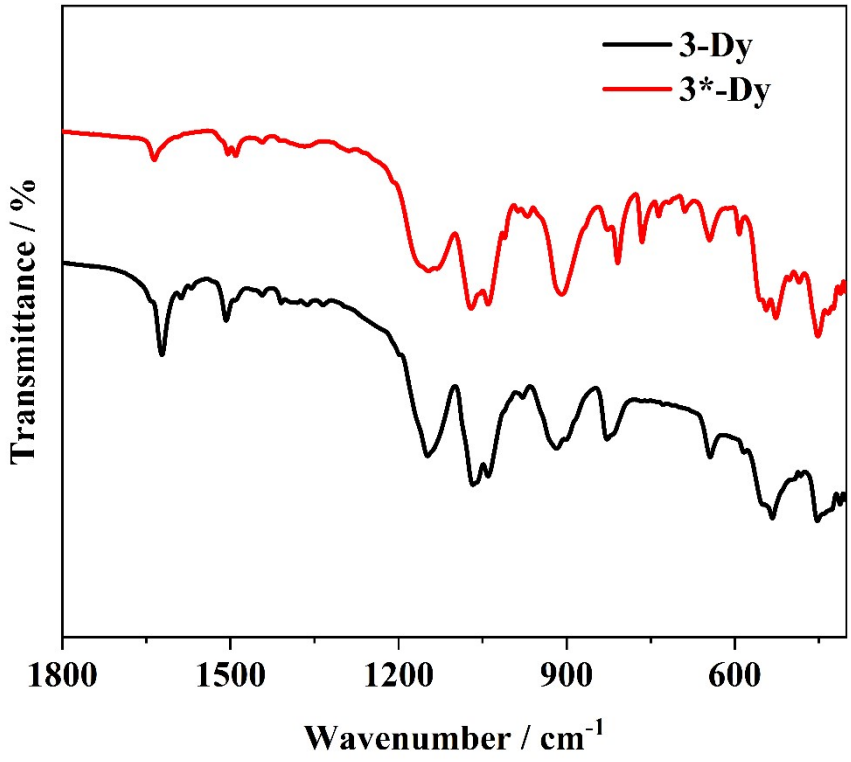

Fig. S40 Room-temperature IR spectra of **3-Dy** and the corresponding irradiated sample **3*-Dy** recorded using a diamond ATR probe.

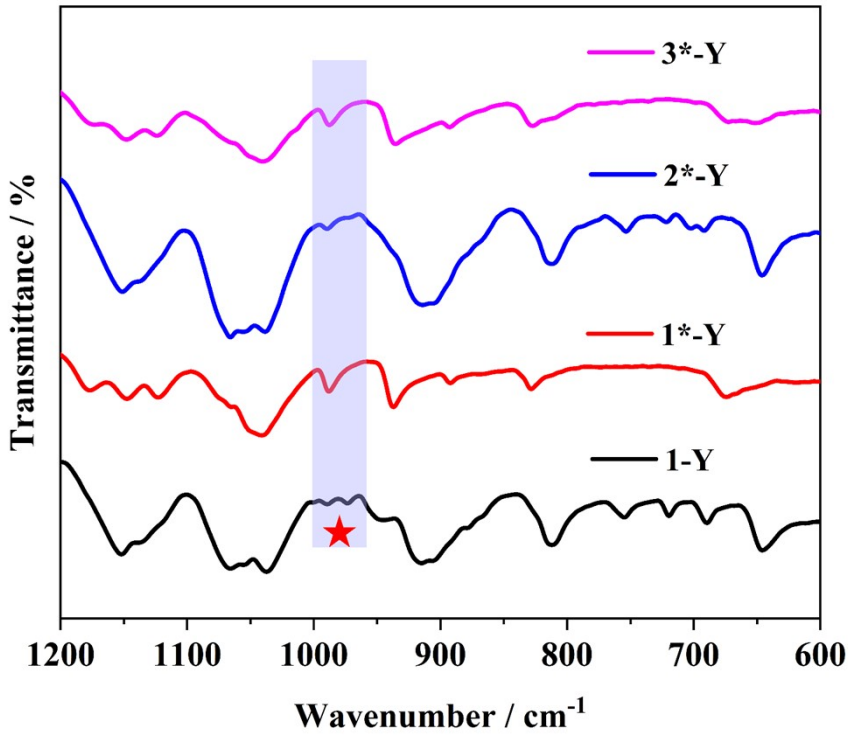

Fig. S41 Room-temperature IR spectra of the irradiated samples with different substituents in the Y series recorded using a diamond ATR probe.

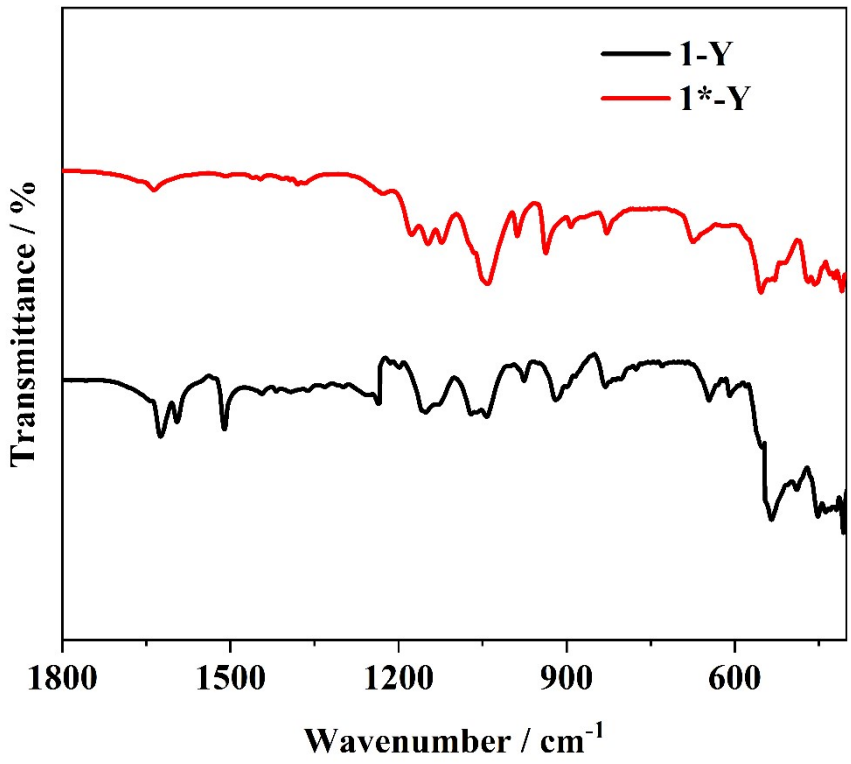

Fig. S42 Room-temperature IR spectra of **1-Y** and the corresponding irradiated sample **1*-Y** recorded using a diamond ATR probe.

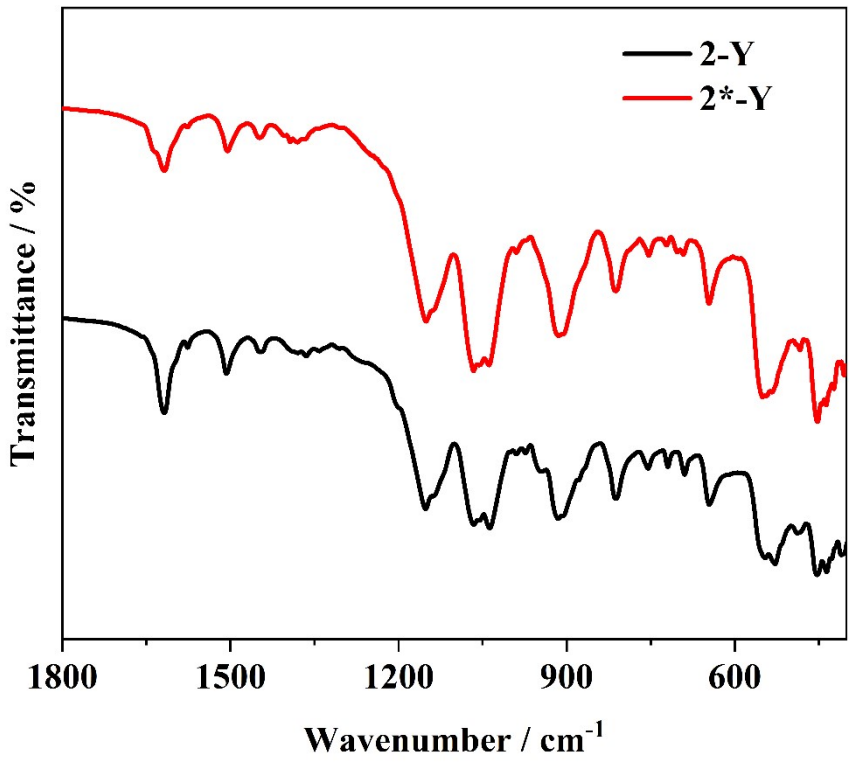

Fig. S43 Room-temperature IR spectra of **2-Y** and the corresponding irradiated sample **2*-Y** recorded using a diamond ATR probe.

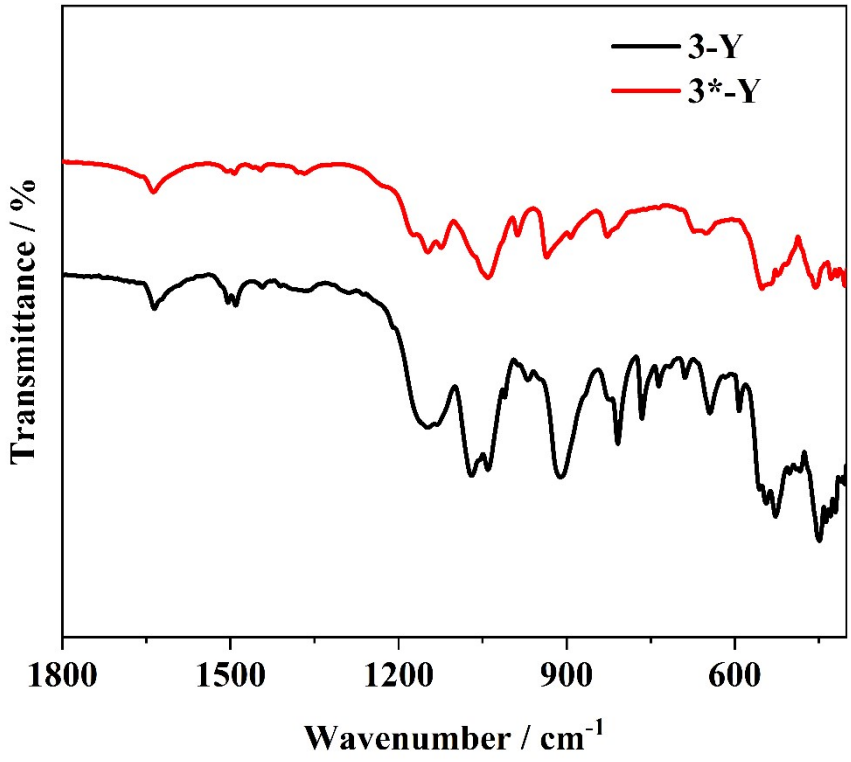

Fig. S44 Room-temperature IR spectra of **3-Y** and the corresponding irradiated sample **3*-Y** recorded using a diamond ATR probe.

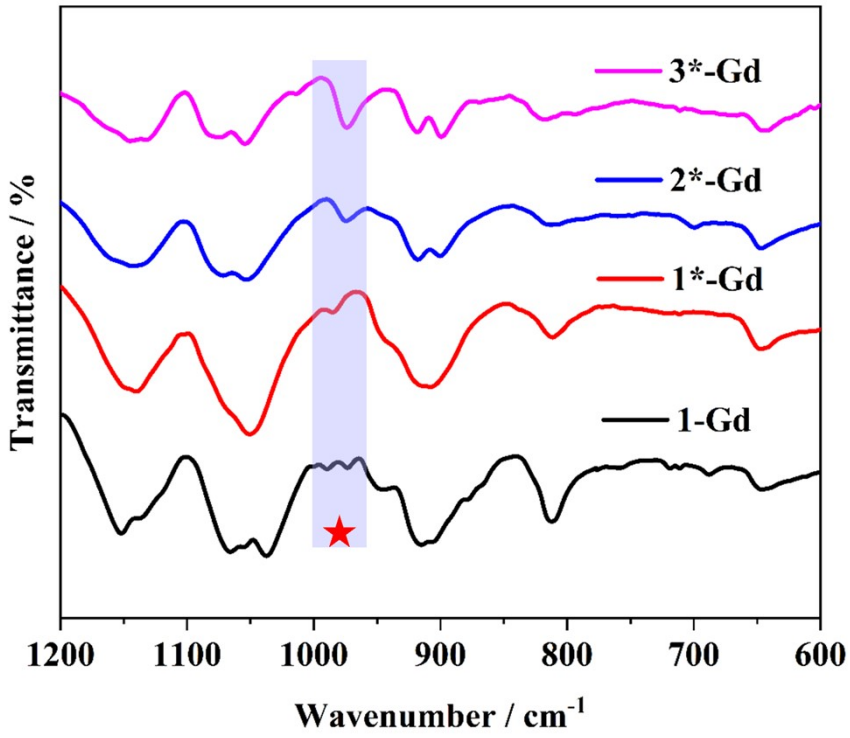

Fig. S45 Room-temperature IR spectra of the irradiated samples with different substituents in the Gd series recorded using a diamond ATR probe.

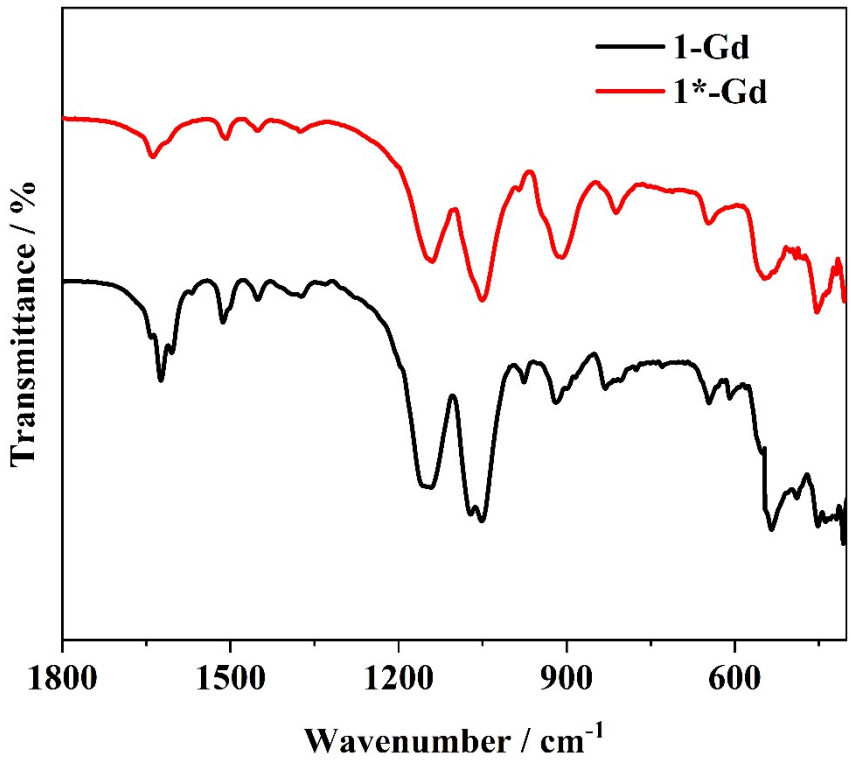

Fig. S46 Room-temperature IR spectra of **1-Gd** and the corresponding irradiated sample **1*-Gd** recorded using a diamond ATR probe.

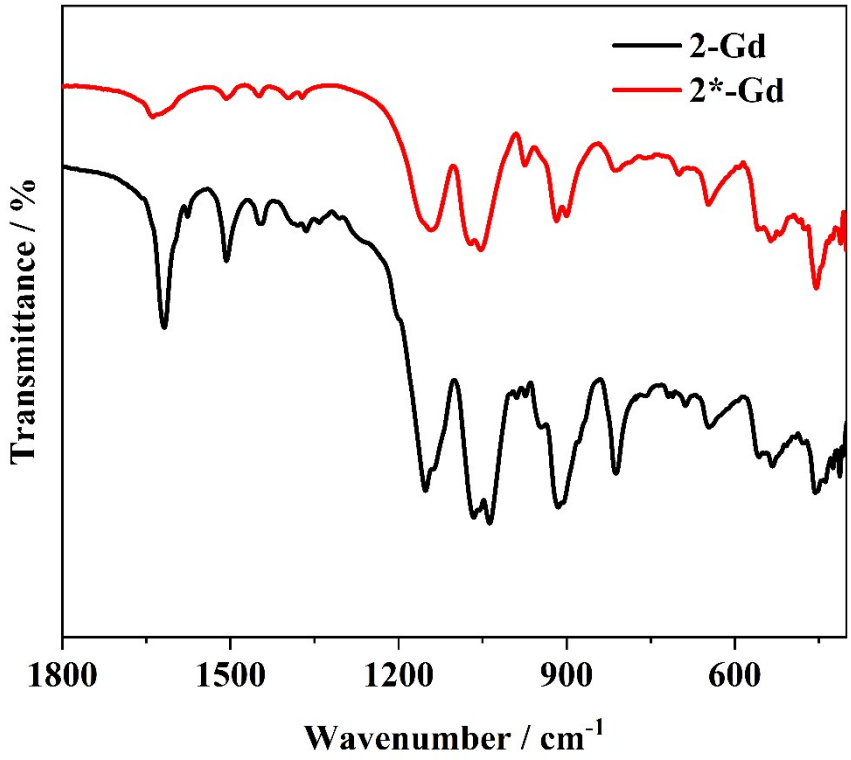

Fig. S47 Room-temperature IR spectra of **2-Gd** and the corresponding irradiated sample **2*-Gd** recorded using a diamond ATR probe.

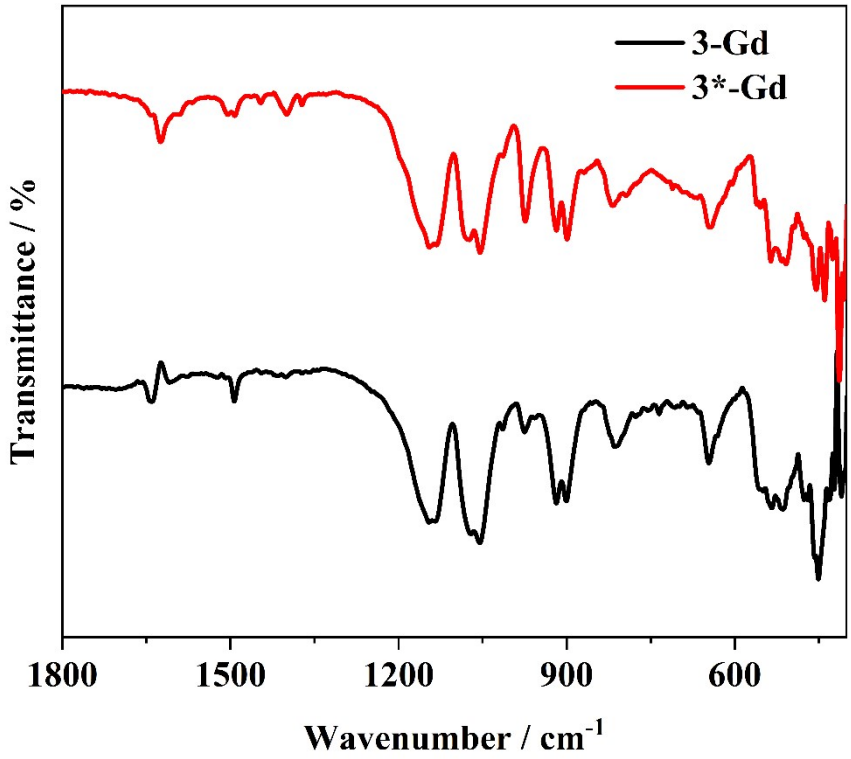

Fig. S48 Room-temperature IR spectra of **3-Gd** and the corresponding irradiated sample **3*-Gd** recorded using a diamond ATR probe.

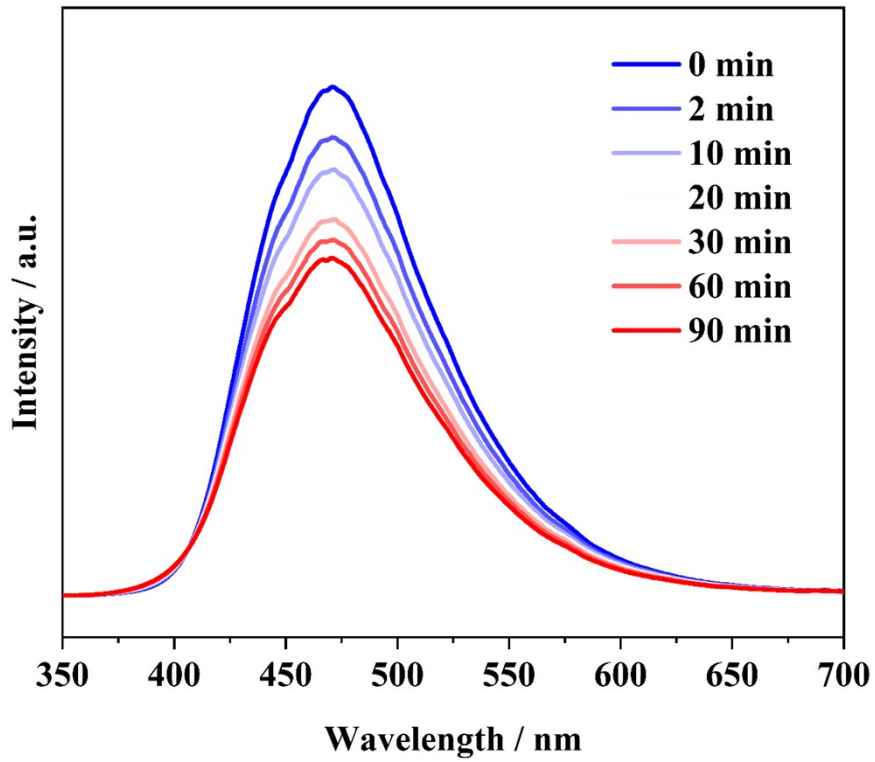

Figure S49 Time-dependent fluorescence intensity spectra of compound **1-Dy**

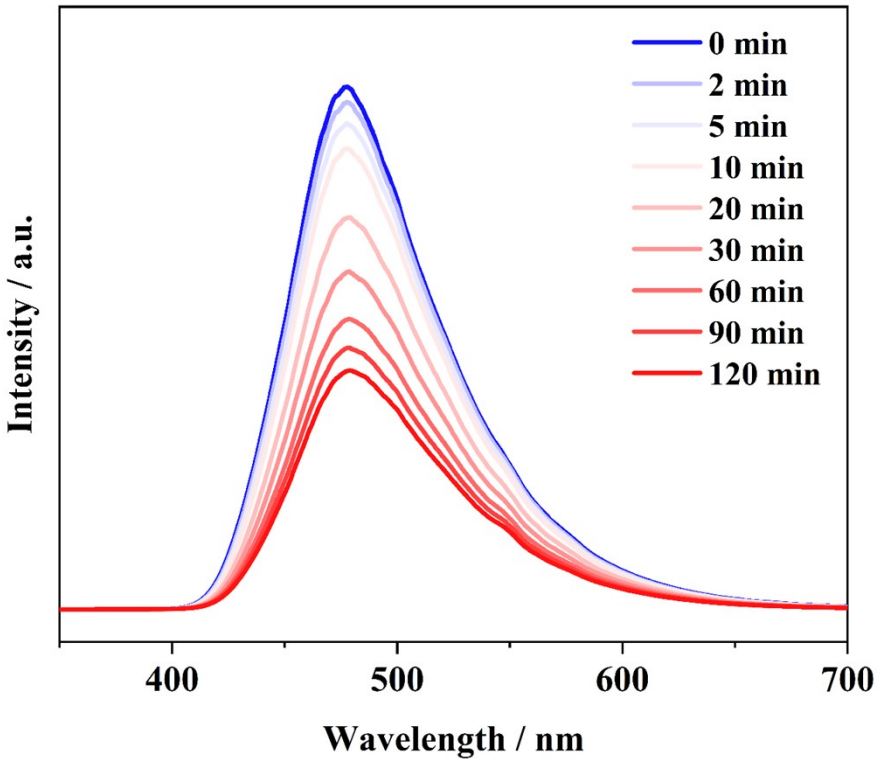

Figure S50 Time-dependent fluorescence intensity spectra of compound **2-Dy.**

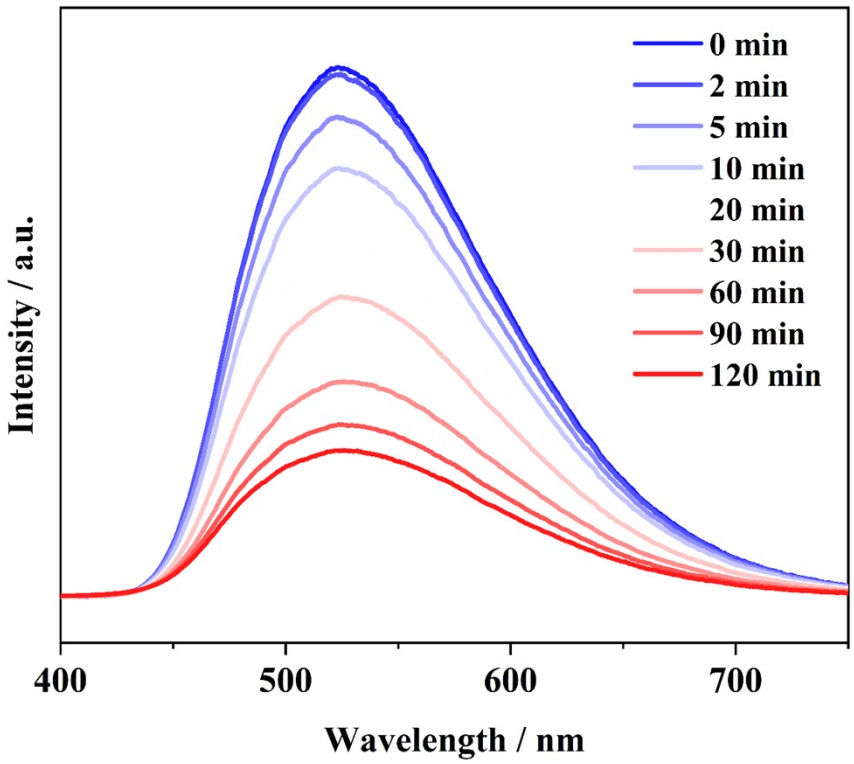

Figure S51 Time-dependent fluorescence intensity spectra of compound **3-Dy.**

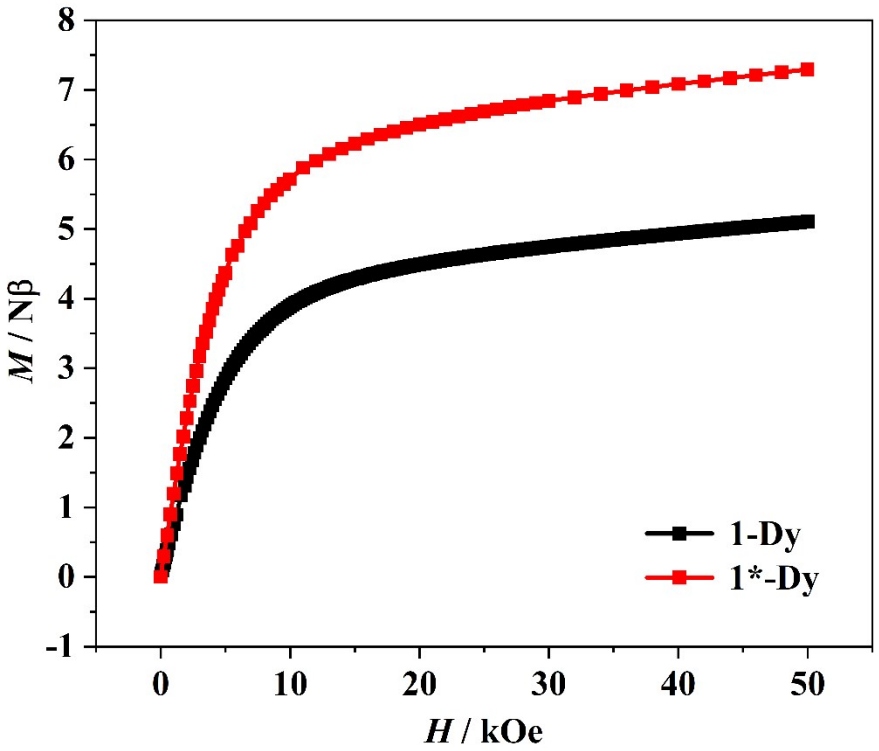

Fig. S52 Isothermal magnetization curves before and after irradiation at 2 K for **1-Dy**.

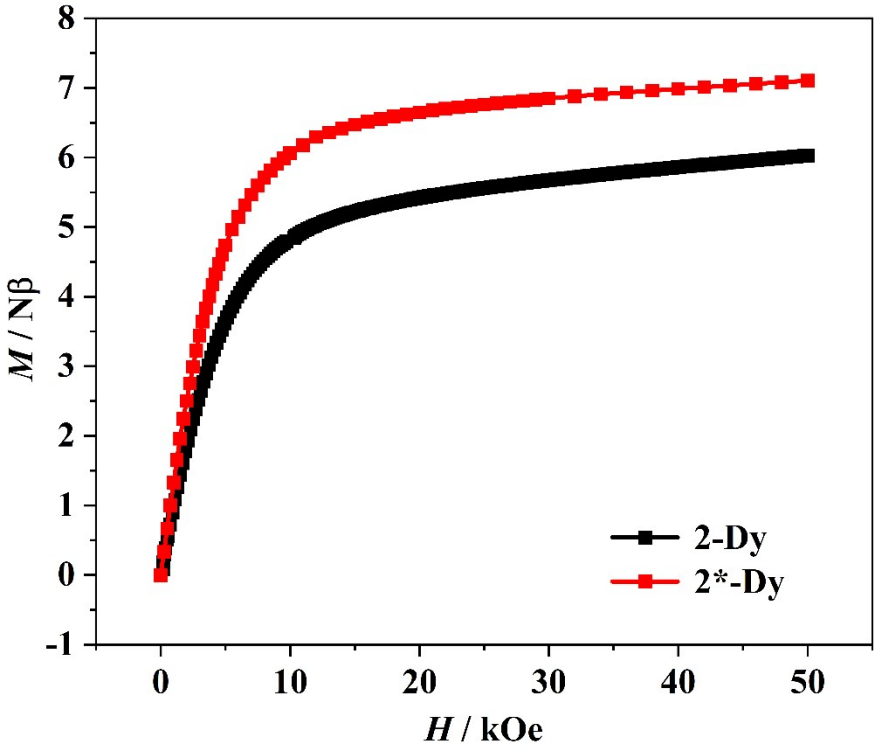

Fig. S53 Isothermal magnetization curves before and after irradiation at 2 K for **2-Dy**.

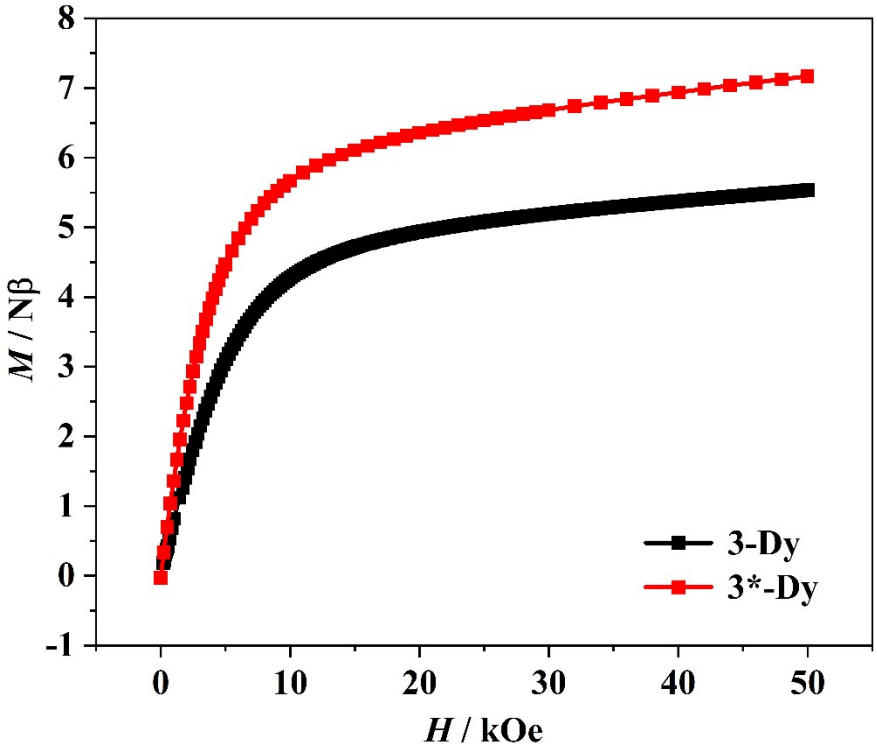

Fig. S54 Isothermal magnetization curves before and after irradiation at 2 K for **3-Dy**.

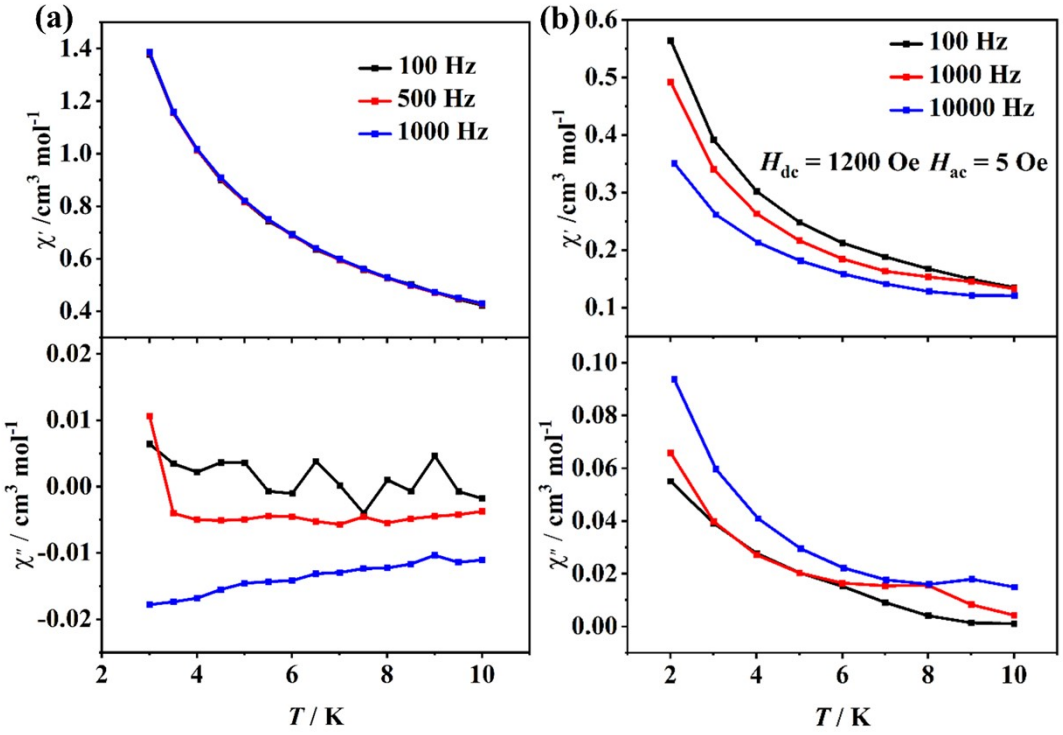

Fig. S55 Temperature dependence of the χ' and χ'' components of the ac magnetic susceptibility for **1-Dy** measured at various ac frequencies under zero dc field (a) and under the optimal dc field (b).

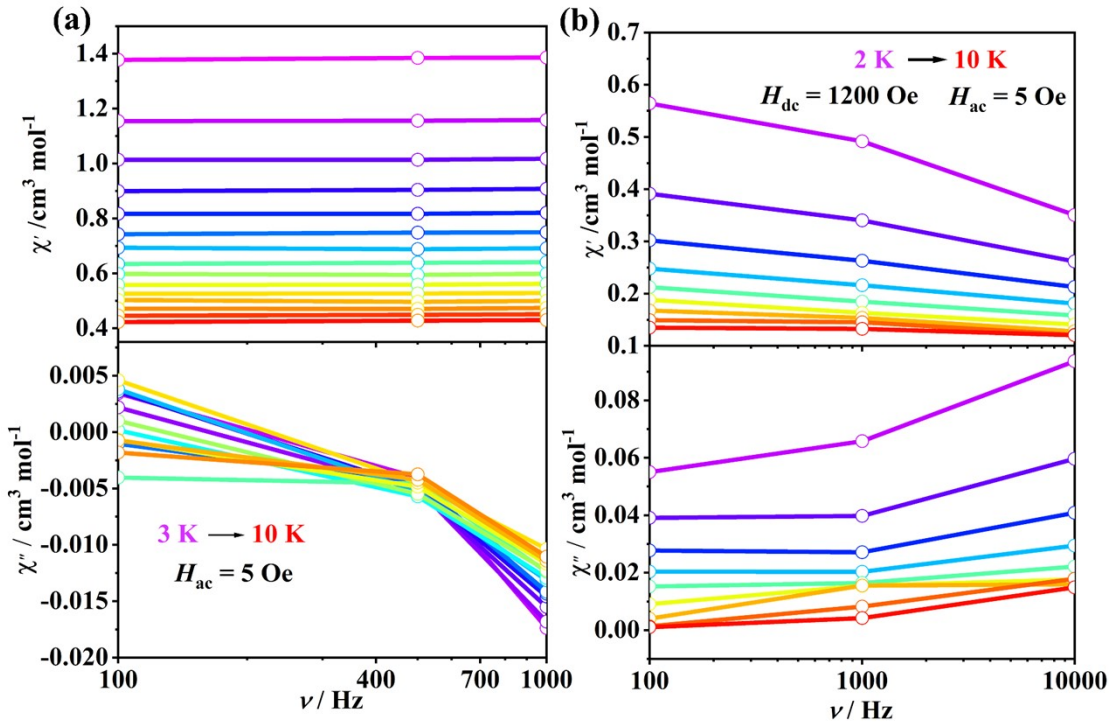

Fig. S56 The frequency dependent χ' and χ'' signals of **1-Dy** measured under 0 Oe dc and 5 Oe ac fields (a) and under 1200 Oe dc and 5 Oe ac fields (b).

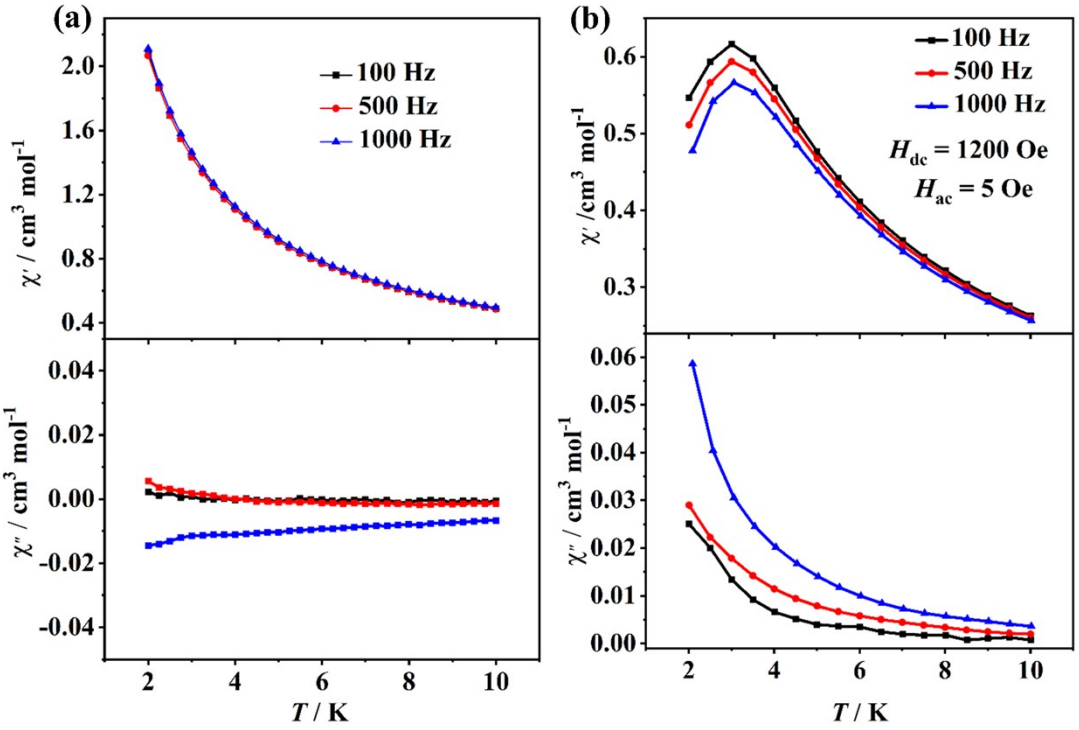

Fig. S57 Temperature dependence of the χ' and χ'' components of the ac magnetic susceptibility for **2-Dy** measured at various ac frequencies under zero dc field (a) and under the optimal dc field (b).

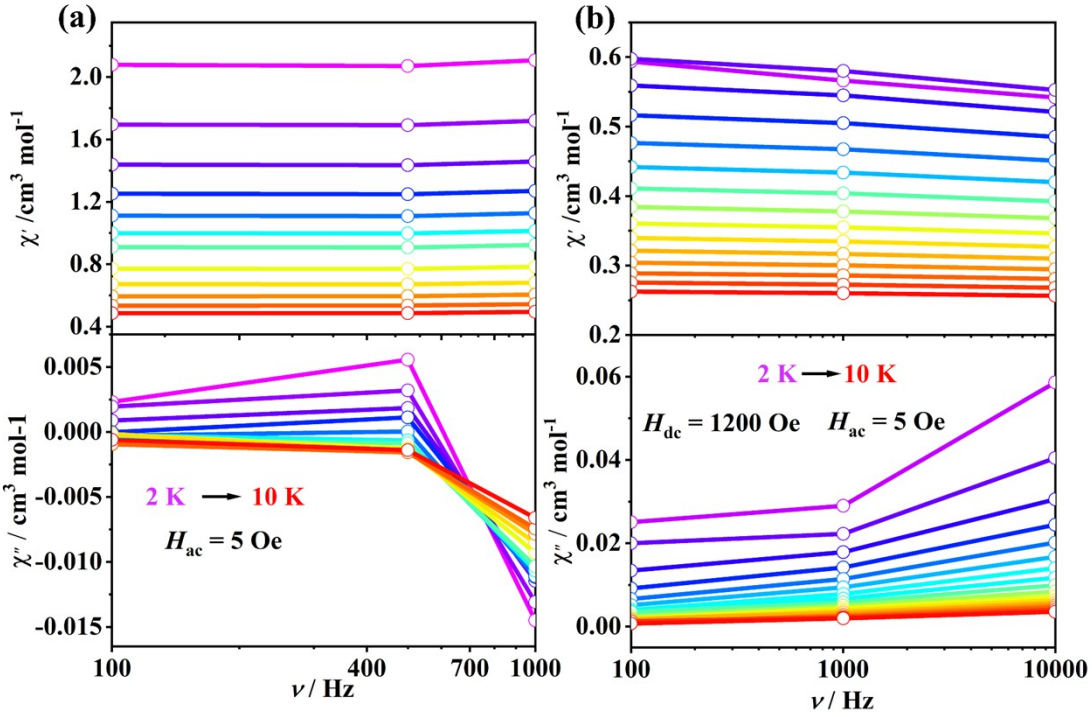

Fig. S58 The frequency dependent χ' and χ'' signals of **2-Dy** measured under 0 Oe dc and 5 Oe ac fields (a) and under 1200 Oe dc and 5 Oe ac fields (b)

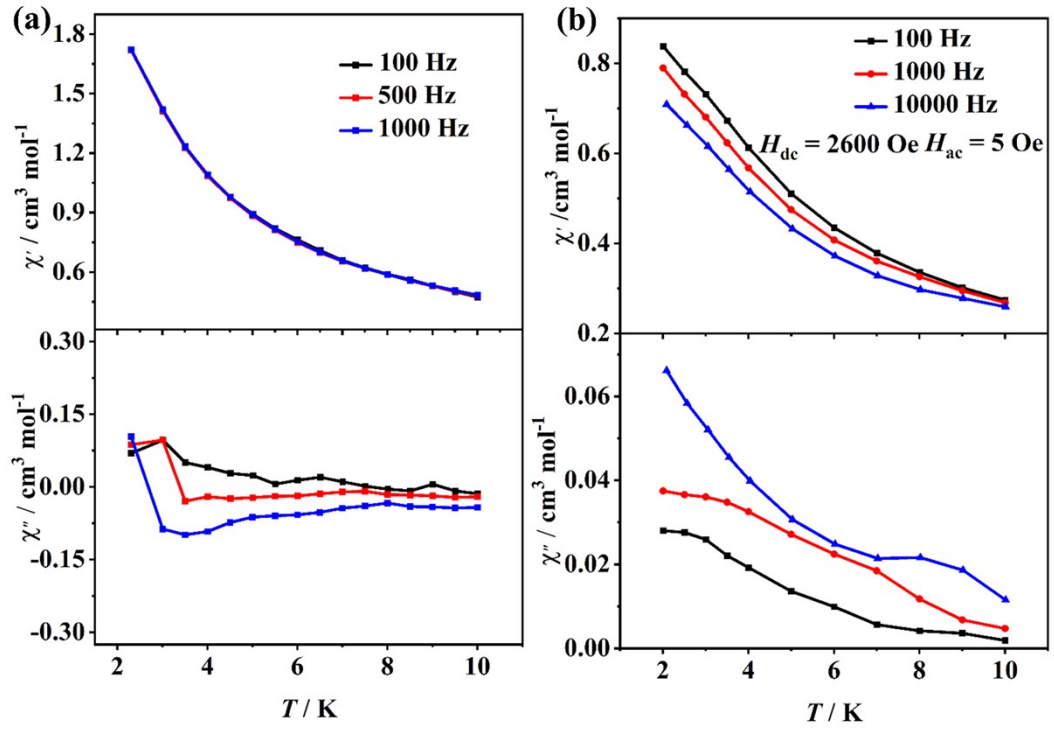

Fig. S59 Temperature dependence of the χ' and χ'' components of the ac magnetic susceptibility for **3-Dy** measured at various ac frequencies under zero dc field (a) and under the optimal dc field (b).

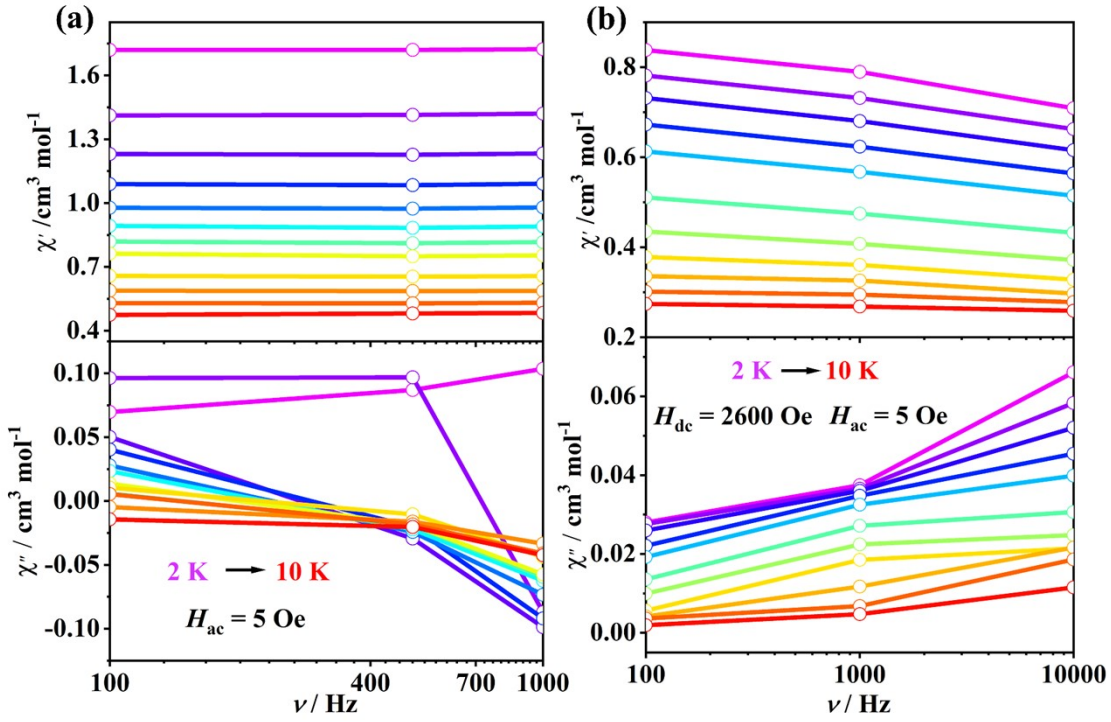

Fig. S60 The frequency dependent χ' and χ'' signals of **3-Dy** measured under 0 Oe dc and 5 Oe ac fields (a) and under 1200 Oe dc and 5 Oe ac fields (b).

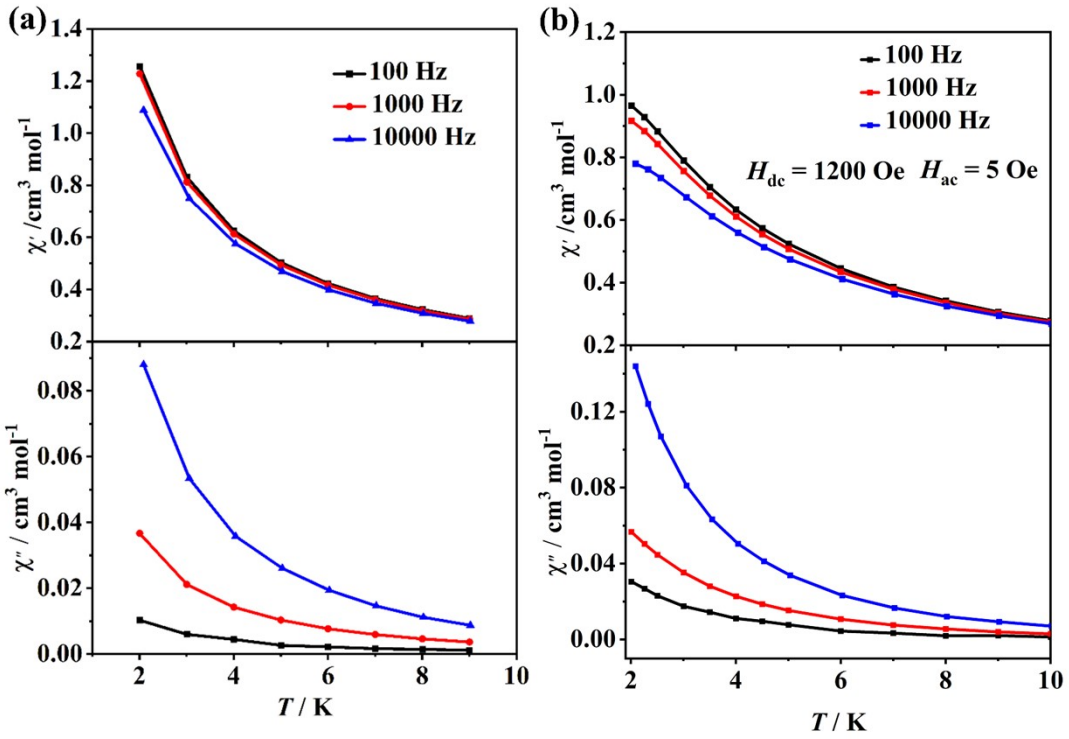

Fig. S61 Temperature dependence of the χ' and χ'' components of the ac magnetic susceptibility for **1*-Dy** measured at various ac frequencies under zero dc field (a) and under the optimal dc field (b).

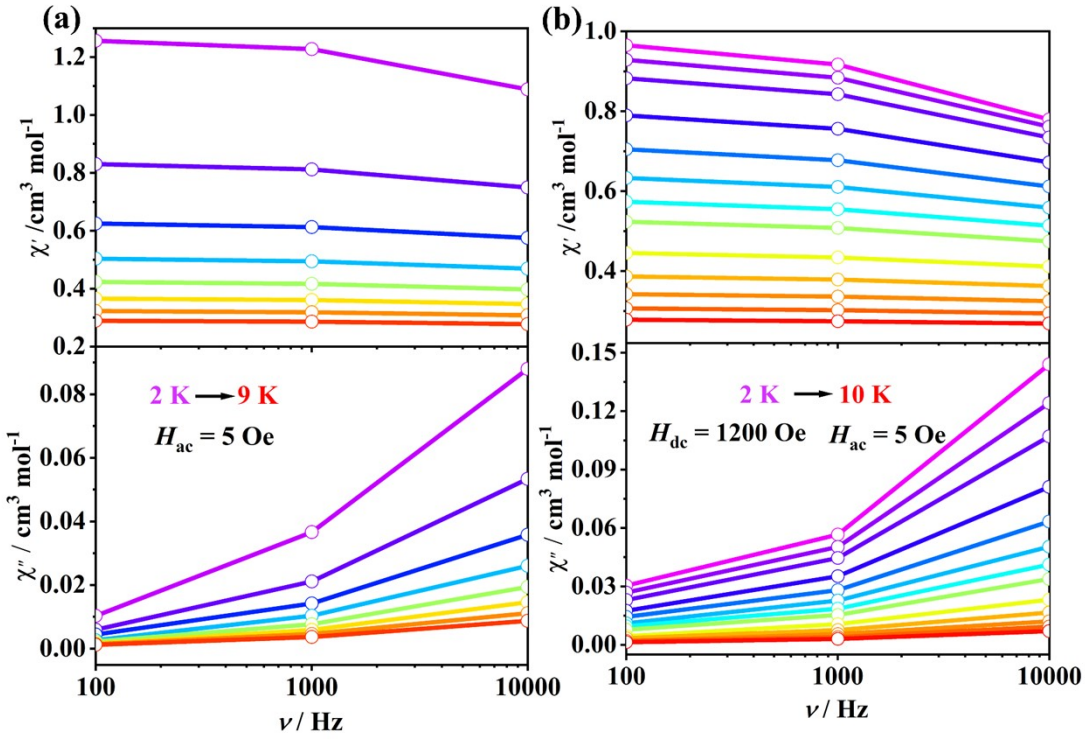

Fig. S62 The frequency dependent χ' and χ'' signals of **1*-Dy** measured under 0 Oe dc and 5 Oe ac fields (a) and under 1200 Oe dc and 5 Oe ac fields (b).

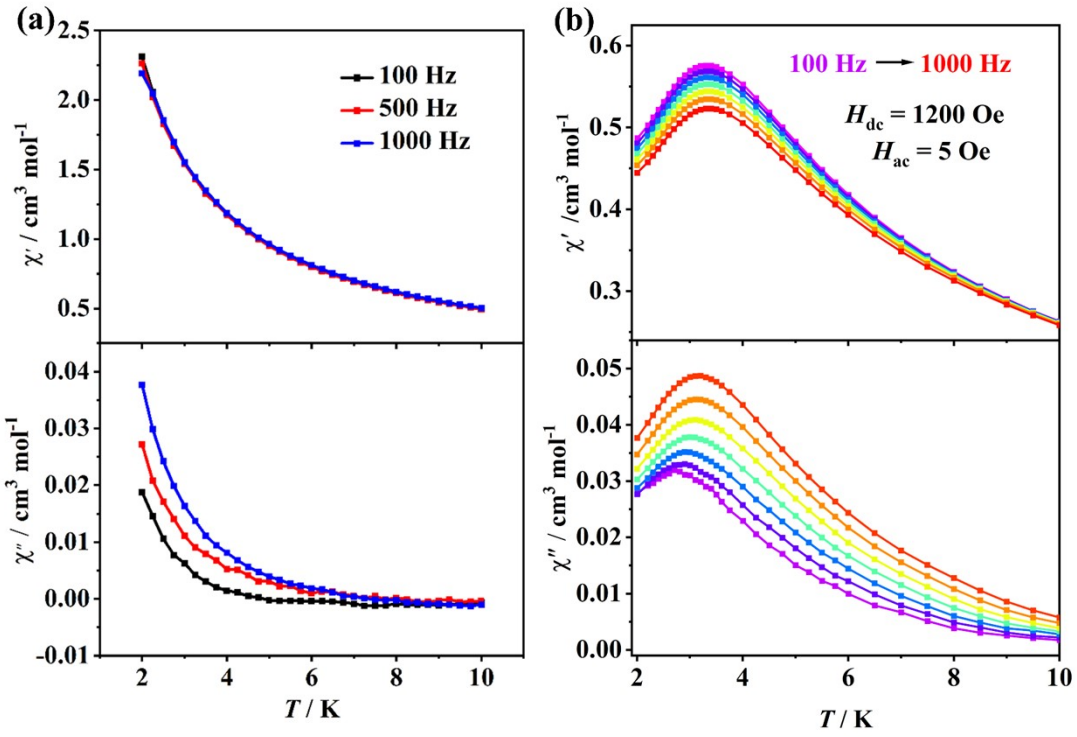

Fig. S63 Temperature dependence of the χ' and χ'' components of the ac magnetic susceptibility for **2*-Dy** measured at various ac frequencies under zero dc field (a) and under the optimal dc field (b).

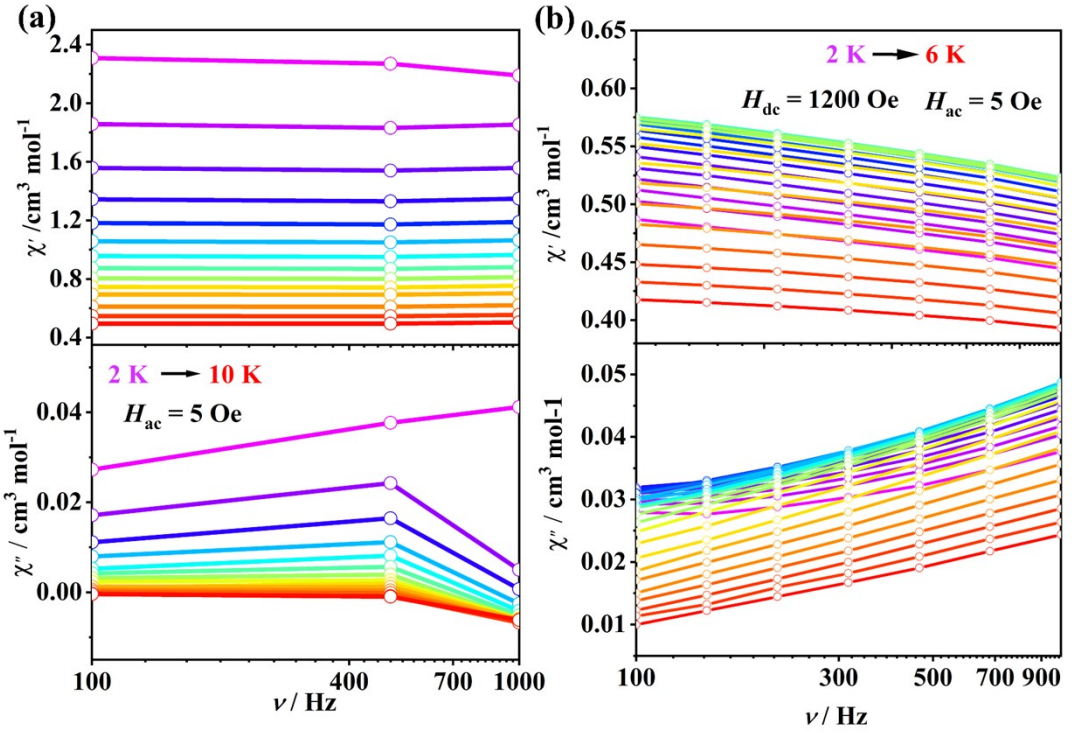

Fig. S64 The frequency dependent χ' and χ'' signals of **2*-Dy** measured under 0 Oe dc and 5 Oe ac fields (a) and under 1200 Oe dc and 5 Oe ac fields (b).

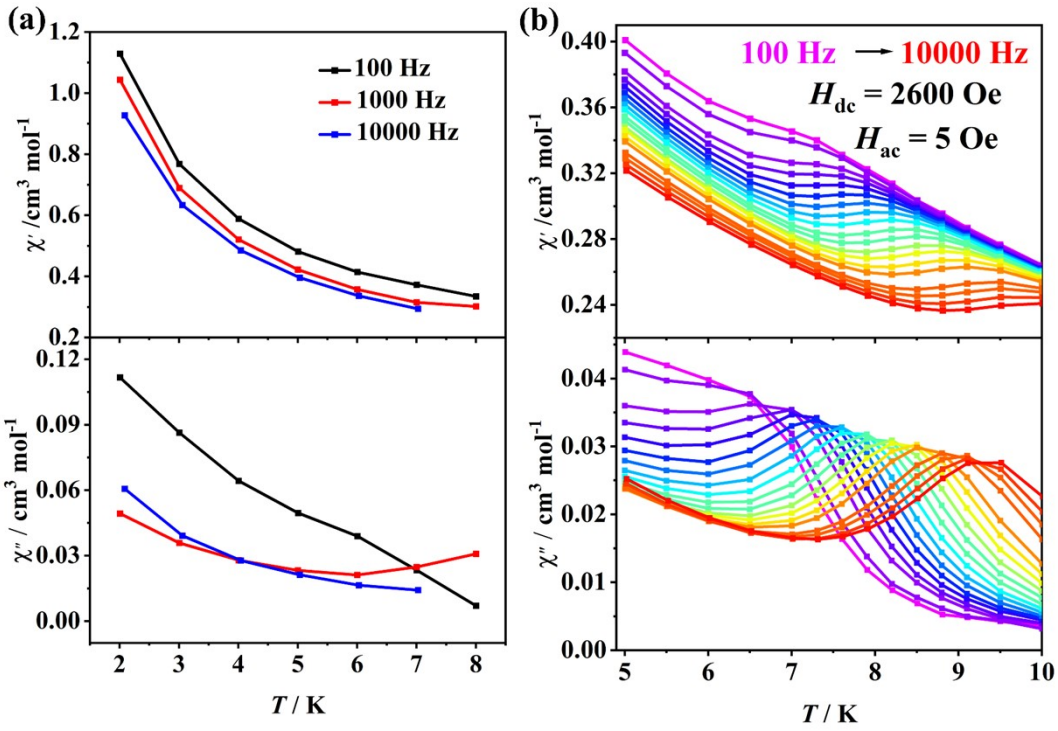

Fig. S65 Temperature dependence of the χ' and χ'' components of the ac magnetic susceptibility for **3*-Dy** measured at various ac frequencies under zero dc field (a) and under the optimal dc field (b).

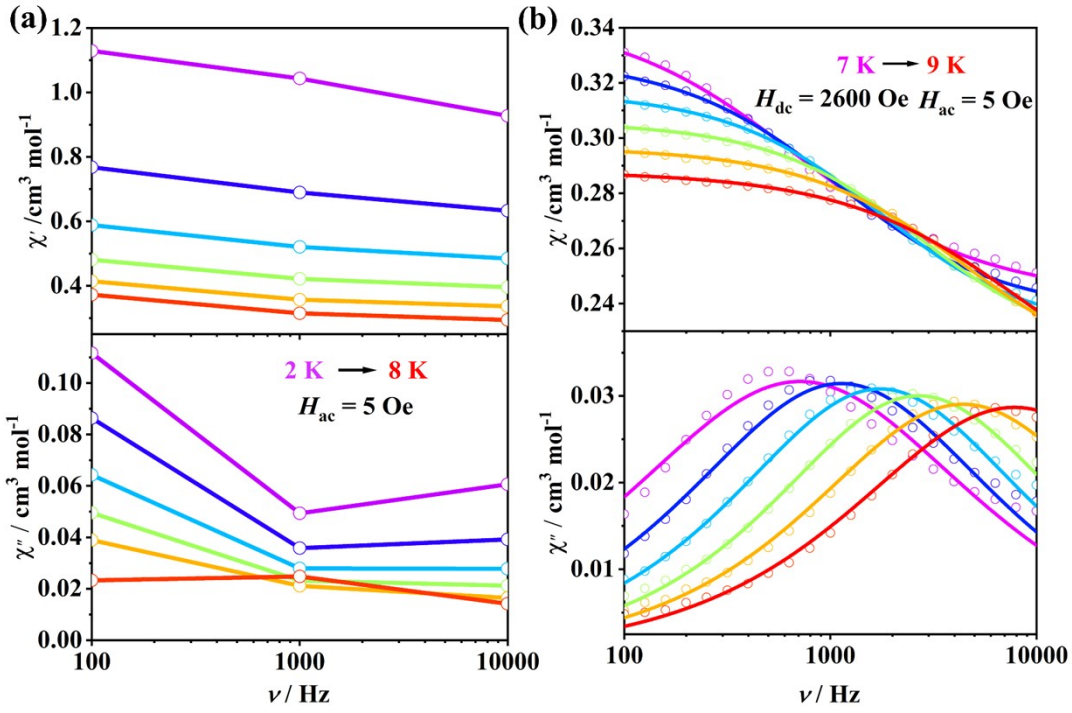

Fig. S66 The frequency dependent χ' and χ'' signals of **3*-Dy** measured under 0 Oe dc and 5 Oe ac fields (a). The frequency dependent χ' and χ'' signals of **3*-Dy** measured under a 2600 Oe dc field and a 5 Oe ac field in the 7.6–9.1 K temperature range (b).

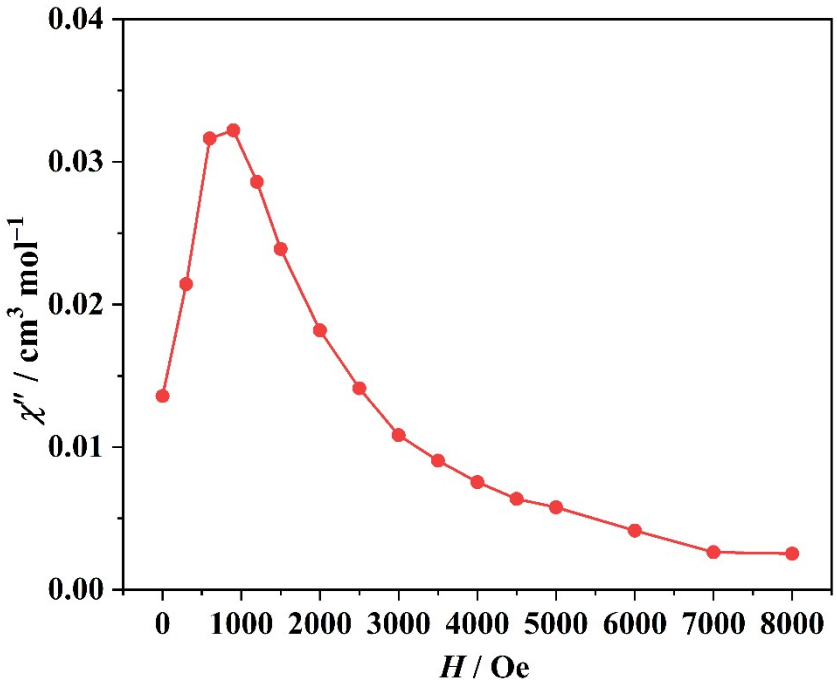

Fig. S67 Field dependence of the χ'' component of ac susceptibility components after irradiation with ω = 100 Hz at 2 K of **2*-Dy**.

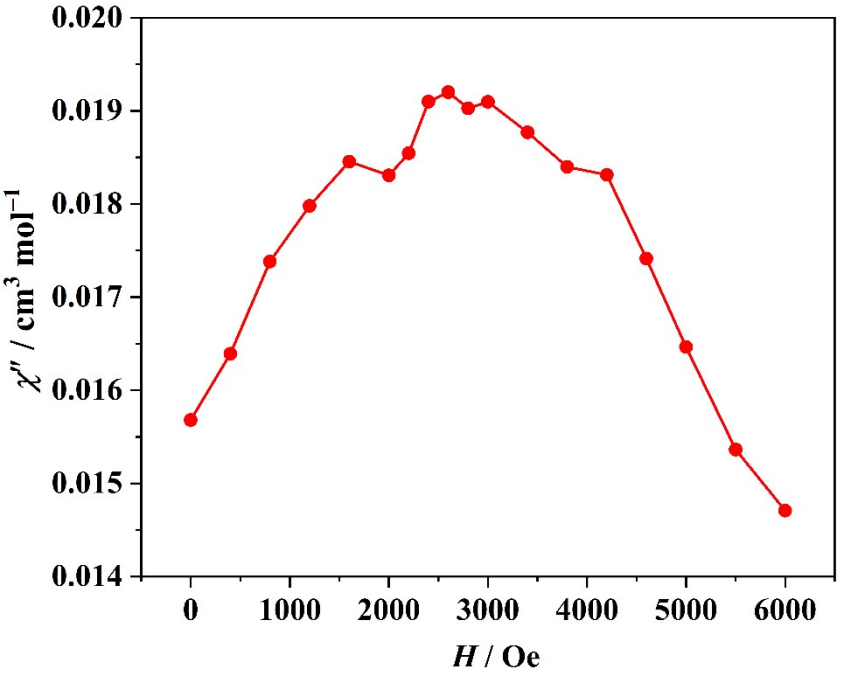

Fig. S68 Field dependence of the χ'' component of ac susceptibility components after irradiation with ω = 1000 Hz at 2 K of **3*-Dy**.

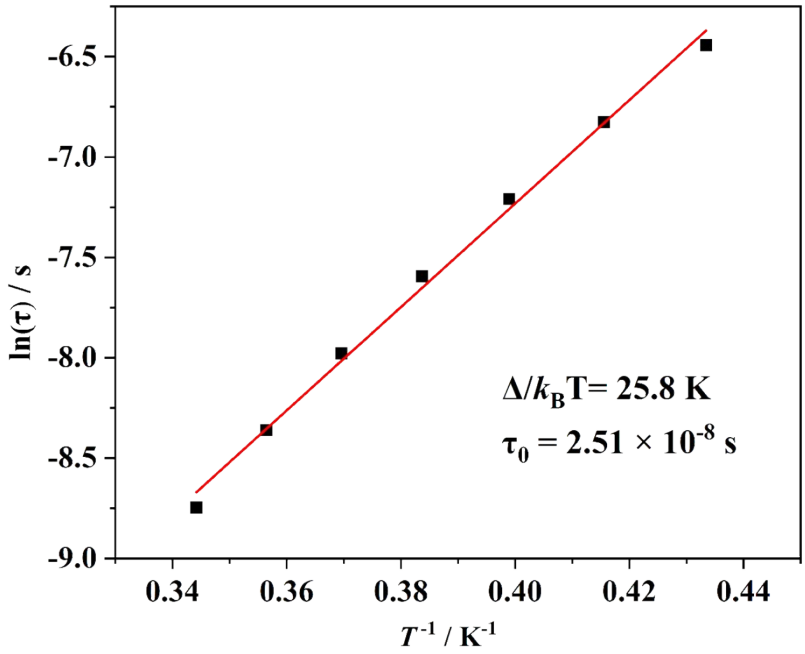

Fig. S69 Arrhenius plots for the magnetic relaxation process after irradiation based on the peak values of χ'' in the temperature-dependent ac susceptibility data of **2*-Dy**. The red full line corresponds to a linear fit.

Table S1. Crystallographic data for **1-Dy**, **2-Dy**, and **3-Dy**.

	1-Dy	**2-Dy**	**3-Dy**
Formula	$C_{18}H_{24}NO_{14}P_4Dy$	$C_{17}H_{24}NO_{14}P_4Dy$	$C_{17}H_{24}ClDyNO_{14}P_4$
*M*r (g·mol^{-1})	764.76	752.75	788.20
Space group	*P*-1	*P*-1	*P*-1
Crystal system	Triclinic	Triclinic	Triclinic
a (Å)	10.5311(2)	10.5071(2)	10.5188(4)
b (Å)	10.5810(2)	10.5386(2)	10.7462(5)
c (Å)	15.6015(3)	15.8382(3)	15.3229(6)
α (°)	74.3990(10)	76.939(2)	77.130(4)
β (°)	75.4030(10)	72.093(2)	76.471(3)
γ (°)	86.6220(10)	86.413(1)	87.652(4)
V (Å^3)	1620.30(5)	1625.59(6)	1641.58(12)
Z	2	2	2
F (000)	754.0	742	776
D_c (g cm^{-3})	1.568	1.538	1.595

μ (mm^{-1})	14.724		2.550		2.608	
R_{int}	0.1008		0.0380		0.0595	
limiting indices	-12<=*h*<=10 -12<=*k*<=12 -18<=*l*<=18		-12<=*h*<=12 -11<=*k*<=12 -18<=*l*<=18		-12<=*h*<=12 -12<=*k*<=12 -17<=*l*<=17	
Collectedreflections	18932		16698		15851	
Unique reflections	5386		5860		5294	
GOF on F^2	1.067		1.108		1.042	
R_1, wR_2 [$I>2\sigma(I)$][a]	0.0642	0.1742	0.0274	0.0720	0.0458	0.1102
R_1, wR_2 [all data][b]	0.0660	0.1765	0.0293	0.0729	0.0567	0.1190

[a]$R_1 = \sum ||F_o| - |F_c||/\sum|F_o|$. [b]$wR_2 = \{\sum[w(F_o^2 - F_c^2)^2]/\sum w(F_o^2)^2\}^{1/2}$.

Table S2. Selected bond lengths (Å) and angles (°) for **1-Dy** at 150 K.

1-Dy			
Dy(1)-O(6)#1	2.362(4)	P(2)-C(14)	1.846(8)
Dy(1)-O(5)	2.250(5)	O(4)-C(14)	1.451(9)
Dy(1)-O(12)#2	2.329(5)	O(13)-C(15)	1.423(9)
Dy(1)-O(11)	2.304(4)	N(1)-C(5)	1.349(12)
Dy(1)-O(3)#1	2.329(5)	N(1)-C(1)	1.323(12)
Dy(1)-O(8)	2.326(5)	C(18)-C(11)	1.340(12)
Dy(1)-O(10)#2	2.329(5)	C(14)-C(16)	1.526(10)
P(1)-O(6)	1.523(5)	C(15)-C(17)	1.524(11)
P(1)-O(5)	1.492(5)	C(3)-C(4)	1.409(12)
P(1)-O(7)	1.570(5)	C(3)-C(2)	1.386(13)
P(1)-C(14)	1.835(7)	C(3)-C(6)	1.469(12)
P(4)-O(12)	1.507(5)	C(5)-C(4)	1.374(12)
P(4)-O(11)	1.509(5)	C(1)-C(2)	1.364(12)
P(4)-O(14)	1.559(5)	C(8)-C(7)	1.469(12)
P(4)-C(15)	1.846(7)	C(8)-C(9)	1.387(15)
P(3)-O(8)	1.513(5)	C(8)-C(13)	1.402(14)
P(3)-O(10)	1.509(5)	C(6)-C(7)	1.310(14)
P(3)-O(9)	1.560(5)	C(9)-C(10)	1.381(13)
P(3)-C(15)	1.825(7)	C(12)-C(13)	1.376(13)
P(2)-O(2)	1.574(5)	C(12)-C(11)	1.376(17)
P(2)-O(3)	1.503(5)	C(10)-C(11)	1.369(17)
P(2)-O(1)	1.502(5)		

O(5)-Dy(1)-O(6)#1	79.52(17)	O(1)-P(2)-O(2)	107.1(3)
O(5)-Dy(1)-O(12)#2	156.63(18)	O(1)-P(2)-O(3)	116.4(3)
O(5)-Dy(1)-O(11)	79.26(17)	O(1)-P(2)-C(14)	108.0(3)
O(5)-Dy(1)-O(3)#1	83.93(17)	P(1)-O(6)-Dy(1)#1	142.5(3)
O(5)-Dy(1)-O(8)	111.84(18)	P(1)-O(5)-Dy(1)	154.4(3)
O(5)-Dy(1)-O(10)#2	108.62(18)	P(4)-O(12)-Dy(1)#2	136.0(3)
O(12)#2-Dy(1)-O(6)#1	82.62(16)	P(4)-O(11)-Dy(1)	138.8(3)
O(10)#2-Dy(1)-O(12)#2	80.56(16)	P(2)-O(3)-Dy(1)#1	142.0(3)
O(11)-Dy(1)-O(6)#1	133.63(16)	P(3)-O(8)-Dy(1)	135.4(3)
O(11)-Dy(1)-O(12)#2	124.11(17)	P(3)-O(10)-Dy(1)#2	136.5(3)
O(11)-Dy(1)-O(3)#1	139.05(17)	C(1)-N(1)-C(5)	121.3(7)
O(11)-Dy(1)-O(8)	76.27(16)	P(1)-C(14)-P(2)	112.5(3)
O(11)-Dy(1)-O(10)#2	75.54(17)	O(4)-C(14)-P(1)	109.4(5)
O(3)#1-Dy(1)-O(6)#1	78.10(16)	O(4)-C(14)-P(2)	105.4(5)
O(3)#1-Dy(1)-O(12)#2	77.70(16)	O(4)-C(14)-C(16)	106.7(5)
O(3)#1-Dy(1)-O(10)#2	74.98(17)	C(16)-C(14)-P(1)	110.1(5)
O(8)-Dy(1)-O(6)#1	74.25(17)	C(16)-C(14)-P(2)	112.3(5)
O(8)-Dy(1)-O(12)#2	77.19(16)	P(3)-C(15)-P(4)	107.8(3)
O(8)-Dy(1)-O(3)#1	144.58(16)	O(13)-C(15)-P(4)	110.3(5)
O(8)-Dy(1)-O(10)#2	124.36(18)	O(13)-C(15)-P(3)	109.2(5)
O(10)#2-Dy(1)-O(6)#1	150.70(15)	O(13)-C(15)-C(17)	107.5(5)
O(6)-P(1)-O(7)	108.1(3)	C(17)-C(15)-P(4)	110.5(5)
O(6)-P(1)-C(14)	108.3(3)	C(17)-C(15)-P(3)	111.5(5)
O(5)-P(1)-O(6)	116.0(3)	C(4)-C(3)-C(6)	124.9(9)

O(5)-P(1)-O(7)	109.1(3)	C(2)-C(3)-C(4)	117.2(8)
O(5)-P(1)-C(14)	109.2(3)	C(2)-C(3)-C(6)	117.9(8)
O(7)-P(1)-C(14)	105.7(3)	N(1)-C(5)-C(4)	119.9(8)
O(12)-P(4)-O(11)	115.9(3)	C(5)-C(4)-C(3)	120.0(8)
O(12)-P(4)-O(14)	108.5(3)	N(1)-C(1)-C(2)	121.2(8)
O(12)-P(4)-C(15)	105.5(3)	C(9)-C(8)-C(7)	116.9(9)
O(11)-P(4)-O(14)	111.0(3)	C(9)-C(8)-C(13)	118.5(8)
O(11)-P(4)-C(15)	108.6(3)	C(13)-C(8)-C(7)	124.6(9)
O(14)-P(4)-C(15)	106.8(3)	C(1)-C(2)-C(3)	120.4(8)
O(8)-P(3)-O(9)	109.8(3)	C(7)-C(6)-C(3)	125.1(9)
O(8)-P(3)-C(15)	110.0(3)	C(6)-C(7)-C(8)	126.5(9)
O(10)-P(3)-O(8)	115.7(3)	C(10)-C(9)-C(8)	121.5(10)
O(10)-P(3)-O(9)	107.2(3)	C(13)-C(12)-C(11)	118.9(9)
O(10)-P(3)-C(15)	106.5(3)	C(11)-C(10)-C(9)	118.1(11)
O(9)-P(3)-C(15)	107.1(3)	C(12)-C(13)-C(8)	120.4(10)
O(2)-P(2)-C(14)	107.4(3)	C(18)-C(11)-C(12)	118.7(10)
O(3)-P(2)-O(2)	111.5(3)	C(18)-C(11)-C(10)	118.7(11)
O(3)-P(2)-C(14)	106.1(3)	C(10)-C(11)-C(12)	122.6(9)

Table S3. Selected bond lengths (Å) and angles (°) for **2-Dy** at 150 K.

2-Dy			
Dy(1)-O(3)#1	2.329(2)	P(4)-O(10)	1.517(2)
Dy(1)-O(5)	2.239(2)	P(4)-C(15)	1.828(4)
Dy(1)-O(7)#1	2.379(2)	O(4)-C(14)	1.455(4)
Dy(1)-O(8)	2.301(2)	O(13)-C(15)	1.445(4)
Dy(1)-O(10)#2	2.318(2)	C(14)-C(16)	1.529(5)
Dy(1)-O(11)	2.332(2)	C(15)-C(17)	1.535(5)
Dy(1)-O(12)#2	2.332(2)	N(1)-C(1)	1.338(6)
P(1)-O(5)	1.494(2)	N(1)-C(5)	1.328(6)
P(1)-O(6)	1.567(2)	C(1)-C(2)	1.331(7)
P(1)-O(7)	1.508(2)	C(2)-C(3)	1.399(7)
P(1)-C(14)	1.831(4)	C(3)-C(4)	1.390(7)
P(2)-O(1)	1.501(3)	C(3)-C(6)	1.467(7)
P(2)-O(2)	1.580(2)	C(4)-C(5)	1.379(6)
P(2)-O(3)	1.506(2)	C(6)-C(7)	1.310(7)
P(2)-C(14)	1.838(4)	C(7)-C(8)	1.490(6)
P(3)-O(11)	1.512(2)	C(8)-C(9)	1.373(7)
P(3)-O(12)	1.514(2)	C(8)-C(13)	1.380(7)
P(3)-O(14)	1.558(3)	C(9)-C(10)	1.371(8)
P(3)-C(15)	1.826(4)	C(10)-C(11)	1.377(9)
P(4)-O(8)	1.501(2)	C(11)-C(12)	1.384(9)
P(4)-O(9)	1.572(2)	C(12)-C(13)	1.357(7)

O(3)#1-Dy(1)-O(7)#1	78.38(8)	O(8)-P(4)-C(15)	108.90(14)
O(3)#1-Dy(1)-O(12)#2	74.73(8)	O(9)-P(4)-C(15)	105.97(15)
O(5)-Dy(1)-O(3)#1	84.19(8)	O(10)-P(4)-O(9)	107.89(14)
O(5)-Dy(1)-O(7)#1	79.67(8)	O(10)-P(4)-C(15)	105.94(14)
O(5)-Dy(1)-O(8)	79.89(8)	P(2)-O(3)-Dy(1)#1	142.34(15)
O(5)-Dy(1)-O(10)#2	156.41(8)	P(1)-O(5)-Dy(1)	155.83(15)
O(5)-Dy(1)-O(11)	110.97(8)	P(1)-O(7)-Dy(1)#1	141.41(14)
O(5)-Dy(1)-O(12)#2	109.68(8)	P(4)-O(8)-Dy(1)	139.25(14)
O(8)-Dy(1)-O(3)#1	138.44(8)	P(4)-O(10)-Dy(1)#2	135.60(14)
O(8)-Dy(1)-O(7)#1	134.68(8)	P(3)-O(11)-Dy(1)	135.40(14)
O(8)-Dy(1)-O(10)#2	123.69(8)	P(3)-O(12)-Dy(1)#2	137.09(14)
O(8)-Dy(1)-O(11)	76.30(8)	P(1)-C(14)-P(2)	112.71(18)
O(8)-Dy(1)-O(12)#2	75.03(8)	O(4)-C(14)-P(1)	109.5(2)
O(10)#2-Dy(1)-O(3)#1	77.77(8)	O(4)-C(14)-P(2)	105.0(2)
O(10)#2-Dy(1)-O(7)#1	81.94(8)	O(4)-C(14)-C(16)	106.7(3)
O(10)#2-Dy(1)-O(11)	77.55(8)	C(16)-C(14)-P(1)	110.5(2)
O(10)#2-Dy(1)-O(12)#2	80.20(8)	C(16)-C(14)-P(2)	112.1(2)
O(11)-Dy(1)-O(3)#1	145.03(8)	P(3)-C(15)-P(4)	108.19(17)
O(11)-Dy(1)-O(7)#1	74.06(8)	O(13)-C(15)-P(3)	108.6(2)
O(11)-Dy(1)-O(12)#2	124.27(8)	O(13)-C(15)-P(4)	109.9(2)
O(12)#2-Dy(1)-O(7)#1	150.24(8)	O(13)-C(15)-C(17)	107.5(3)
O(5)-P(1)-O(6)	109.41(13)	C(17)-C(15)-P(3)	111.7(2)
O(5)-P(1)-O(7)	116.38(14)	C(17)-C(15)-P(4)	110.9(2)
O(5)-P(1)-C(14)	108.62(15)	C(1)-N(1)-C(5)	121.2(4)
O(6)-P(1)-C(14)	105.70(15)	N(1)-C(1)-C(2)	121.7(5)

O(7)-P(1)-O(6)	107.38(13)	C(1)-C(2)-C(3)	119.4(5)
O(7)-P(1)-C(14)	108.81(15)	C(2)-C(3)-C(4)	118.5(4)
O(1)-P(2)-O(2)	107.57(14)	C(2)-C(3)-C(6)	115.3(5)
O(1)-P(2)-O(3)	115.86(14)	C(4)-C(3)-C(6)	126.2(5)
O(1)-P(2)-C(14)	108.10(16)	C(5)-C(4)-C(3)	118.9(4)
O(2)-P(2)-C(14)	107.57(14)	N(1)-C(5)-C(4)	120.3(4)
O(3)-P(2)-O(2)	111.41(14)	C(7)-C(6)-C(3)	124.4(5)
O(3)-P(2)-C(14)	106.00(15)	C(6)-C(7)-C(8)	126.4(5)
O(11)-P(3)-O(14)	110.15(13)	C(9)-C(8)-C(7)	116.8(5)
O(11)-P(3)-C(15)	109.14(14)	C(9)-C(8)-C(13)	118.2(4)
O(12)-P(3)-O(11)	115.88(13)	C(13)-C(8)-C(7)	124.9(4)
O(12)-P(3)-O(14)	107.97(14)	C(10)-C(9)-C(8)	121.7(5)
O(12)-P(3)-C(15)	106.32(14)	C(9)-C(10)-C(11)	118.9(5)
O(14)-P(3)-C(15)	107.27(15)	C(10)-C(11)-C(12)	120.3(5)
O(8)-P(4)-O(9)	111.66(13)	C(13)-C(12)-C(11)	119.4(5)
O(8)-P(4)-O(10)	115.89(14)	C(12)-C(13)-C(8)	121.5(5)

Table S4. Selected bond lengths (Å) and angles (°) for **3-Dy** at 100 K.

3-Dy			
Dy(1)-O(5)	2.212(4)	Cl(1)-C(11)	1.733(9)
Dy(1)-O(12)#1	2.325(4)	O(4)-C(14)	1.466(8)
Dy(1)-O(8)	2.307(5)	O(13)-C(15)	1.439(8)
Dy(1)-O(7)#2	2.381(4)	N(1)-C(5)	1.330(10)
Dy(1)-O(11)	2.317(5)	N(1)-C(1)	1.327(12)
Dy(1)-O(3)#2	2.325(4)	C(14)-C(16)	1.530(9)
Dy(1)-O(10)#1	2.324(5)	C(15)-C(17)	1.519(10)
P(1)-O(5)	1.500(4)	C(5)-C(4)	1.355(12)
P(1)-O(7)	1.492(5)	C(11)-C(10)	1.367(13)
P(1)-O(6)	1.567(5)	C(11)-C(12)	1.352(14)
P(1)-C(14)	1.821(7)	C(4)-C(3)	1.388(16)
P(3)-O(12)	1.498(5)	C(9)-C(8)	1.375(13)
P(3)-O(11)	1.506(5)	C(9)-C(10)	1.372(12)
P(3)-O(14)	1.561(5)	C(8)-C(13)	1.359(16)
P(3)-C(15)	1.823(7)	C(8)-C(7)	1.58(2)
P(4)-O(8)	1.485(5)	C(8)-C(6)	1.37(2)
P(4)-O(10)	1.511(5)	C(12)-C(13)	1.371(16)
P(4)-O(9)	1.556(5)	C(3)-C(2)	1.373(18)
P(4)-C(15)	1.838(8)	C(3)-C(18)	1.435(18)
P(2)-O(3)	1.502(5)	C(3)-C(19)	1.70(4)
P(2)-O(2)	1.571(5)	C(1)-C(2)	1.319(17)
P(2)-O(1)	1.492(5)	C(7)-C(18)	1.29(3)
P(2)-C(14)	1.825(7)	C(6)-C(19)	1.38(3)

O(5)-Dy(1)-O(12)#1	107.55(16)	P(1)-O(5)-Dy(1)	158.0(3)
O(5)-Dy(1)-O(8)	80.08(16)	P(3)-O(12)-Dy(1)#1	137.1(3)
O(5)-Dy(1)-O(7)#2	79.97(15)	P(4)-O(8)-Dy(1)	139.9(3)
O(5)-Dy(1)-O(11)	112.62(16)	P(1)-O(7)-Dy(1)#2	141.9(3)
O(5)-Dy(1)-O(3)#2	83.54(16)	P(3)-O(11)-Dy(1)	135.9(3)
O(5)-Dy(1)-O(10)#1	156.27(1)	P(2)-O(3)-Dy(1)#2	142.1(3)
O(12)#1-Dy(1)-O(7)#2	151.14(16)	P(4)-O(10)-Dy(1)#1	134.7(3)
O(12)#1-Dy(1)-O(3)#2	74.97(15)	C(1)-N(1)-C(5)	121.3(8)
O(12)#1-Dy(1)-O(10)#1	80.81(16)	P(1)-C(14)-P(2)	113.9(4)
O(8)-Dy(1)-O(12)#1	74.70(16)	O(4)-C(14)-P(1)	108.8(4)
O(8)-Dy(1)-O(7)#2	134.04(16)	O(4)-C(14)-P(2)	105.6(4)
O(8)-Dy(1)-O(11)	75.59(16)	O(4)-C(14)-C(16)	106.3(5)
O(8)-Dy(1)-O(3)#2	139.05(15)	C(16)-C(14)-P(1)	109.4(5)
O(8)-Dy(1)-O(10)#1	123.63(15)	C(16)-C(14)-P(2)	112.4(5)
O(11)-Dy(1)-O(12)#1	123.98(15)	P(3)-C(15)-P(4)	107.9(4)
O(11)-Dy(1)-O(7)#2	74.70(15)	O(13)-C(15)-P(3)	108.6(4)
O(11)-Dy(1)-O(3)#2	145.15(16)	O(13)-C(15)-P(4)	109.0(4)
O(11)-Dy(1)-O(10)#1	77.80(16)	O(13)-C(15)-C(17)	107.3(6)
O(3)#2-Dy(1)-O(7)#2	78.38(15)	C(17)-C(15)-P(3)	112.1(5)
O(3)#2-Dy(1)-O(10)#1	77.18(16)	C(17)-C(15)-P(4)	111.8(5)
O(10)#1-Dy(1)-O(7)#2	82.68(15)	N(1)-C(5)-C(4)	119.9(8)
O(5)-P(1)-O(6)	110.5(3)	C(10)-C(11)-Cl(1)	119.2(8)
O(5)-P(1)-C(14)	108.2(3)	C(12)-C(11)-Cl(1)	118.6(8)

O(7)-P(1)-O(5)	115.5(3)	C(12)-C(11)-C(10)	122.2(9)
O(7)-P(1)-O(6)	107.8(3)	C(5)-C(4)-C(3)	119.5(10)
O(7)-P(1)-C(14)	108.2(3)	C(10)-C(9)-C(8)	121.3(9)
O(6)-P(1)-C(14)	106.2(3)	C(9)-C(8)-C(7)	108.8(11)
O(12)-P(3)-O(11)	116.3(3)	C(13)-C(8)-C(9)	118.1(9)
O(12)-P(3)-O(14)	107.5(3)	C(13)-C(8)-C(7)	133.0(12)
O(12)-P(3)-C(15)	106.8(3)	C(13)-C(8)-C(6)	100.4(15)
O(11)-P(3)-O(14)	110.7(3)	C(6)-C(8)-C(9)	141.5(15)
O(11)-P(3)-C(15)	108.4(3)	C(11)-C(10)-C(9)	118.1(8)
O(14)-P(3)-C(15)	106.7(3)	C(11)-C(12)-C(13)	118.3(9)
O(8)-P(4)-O(10)	115.7(3)	C(4)-C(3)-C(18)	135.4(15)
O(8)-P(4)-O(9)	112.7(3)	C(4)-C(3)-C(19)	95.8(14)
O(8)-P(4)-C(15)	108.5(3)	C(2)-C(3)-C(4)	117.7(10)
O(10)-P(4)-O(9)	106.7(3)	C(2)-C(3)-C(18)	106.9(13)
O(10)-P(4)-C(15)	106.4(3)	C(2)-C(3)-C(19)	146.6(14)
O(9)-P(4)-C(15)	106.4(3)	C(2)-C(1)-N(1)	120.7(10)
O(3)-P(2)-O(2)	112.0(3)	C(1)-C(2)-C(3)	120.9(10)
O(3)-P(2)-C(14)	105.6(3)	C(8)-C(13)-C(12)	122.0(9)
O(2)-P(2)-C(14)	107.4(3)	C(18)-C(7)-C(8)	122(2)
O(1)-P(2)-O(3)	116.4(3)	C(7)-C(18)-C(3)	118.3(18)
O(1)-P(2)-O(2)	106.8(3)	C(8)-C(6)-C(19)	115(3)
O(1)-P(2)-C(14)	108.3(3)	C(6)-C(19)-C(3)	111(2)

Table S5. Continuous Shape Measure (CShM) analyses of geometries for **1-Dy** by SHAPE 2.0 Software.

Geometry	**Dy**
Heptagon (D_{7h})	34.408
Hexagonal pyramid (C_{6v})	21.011
Pentagonal bipyramid (D_{5h})	5.438
Capped octahedron (C_{3v})	0.524
Capped trigonal prism J2(C_{2v})	1.162
Johnson pentagonal bipyramid J13 (D_{5h})	8.724
Johnson elongated triangular pyramid J7 (C_{3v})	19.285

Table S6. Continuous Shape Measure (CShM) analyses of geometries for **2-Dy** by SHAPE 2.0 Software.

Geometry	**Dy**
Heptagon (D_{7h})	34.187
Hexagonal pyramid (C_{6v})	21.099
Pentagonal bipyramid (D_{5h})	5.381
Capped octahedron (C_{3v})	0.518
Capped trigonal prism J2(C_{2v})	1.308
Johnson pentagonal bipyramid J13 (D_{5h})	8.535
Johnson elongated triangular pyramid J7 (C_{3v})	19.311

Table S7. Continuous Shape Measure (CShM) analyses of geometries for **3-Dy** by SHAPE 2.0 Software.

Geometry	**Dy**
Heptagon (D_{7h})	34.205
Hexagonal pyramid (C_{6v})	21.181
Pentagonal bipyramid (D_{5h})	5.367
Capped octahedron (C_{3v})	0.573
Capped trigonal prism J2(C_{2v})	1.078
Johnson pentagonal bipyramid J13 (D_{5h})	8.469
Johnson elongated triangular pyramid J7 (C_{3v})	19.165

Table S8. Details of Hydrogen Bond Interactions in **1-Dy** at 150 K.

D–H···A	*d*(D–H) (Å)	*d*(H···A) (Å)	*d*(D···A) (Å)	∠(DHA) (deg)
N1–H1···O1	0.88	1.81	2.674(9)	169
O4–H4···O12	0.84	1.93	2.756(7)	166
O13–H13···O3	0.84	2.14	2.972(7)	171
O13–H13···O12	0.84	2.57	2.986(6)	111

Table S9. Details of Hydrogen Bond Interactions in **2-Dy** at 150 K.

D–H···A	*d*(D–H) (Å)	*d*(H···A) (Å)	*d*(D···A) (Å)	∠(DHA) (deg)
N1–H1···O1	0.82(6)	1.89(6)	2.675(4)	158(6)
O4–H4···O10	0.67(5)	2.06(5)	2.725(4)	176(2)
O13–H13···O3	0.84	2.28	3.007(3)	146
O13–H13···O10	0.84(7)	2.48	2.981(3)	119

Table S10. Details of Hydrogen Bond Interactions in **3-Dy** at 150 K.

D–H···A	*d*(D–H) (Å)	*d*(H···A) (Å)	*d*(D···A) (Å)	∠(DHA) (deg)
N1–H1A···O1	0.88	1.80	2.665(9)	169
O4–H4···O10	0.84	1.92	2.758(6)	171
O13–H13···O3	0.84	2.10	2.939(6)	176
O13–H13···O10	0.84	2.59	2.967(6)	109

Table S11 The Cole-Cole fitting parameters of **3*-Dy** from 7.6 K to 9.1 K based on the generalized Debye law.

T	7.6	7.9	8.2	8.5	8.8	9.1
τ	2.23556E-4	1.41165E-4	9.14013E-5	5.93696E-5	3.61323E-5	2.0361E-5
α	0.30984	0.25129	0.22716	0.21767	0.24574	0.2793